Journal of Volcanology and Geothermal Research 342 (2017) 29–46

Contents lists available at ScienceDirect

Journal of Volcanology and Geothermal Research

journal homepage: www.elsevier.com/locate/jvolgeores

Plateaus and sinuous ridges as the fingerprints of lava flow inflation in the Eastern Tharsis Plains of Mars

Jacob E. Bleacher [a,*], Tim R. Orr [b], Andrew P. de Wet [c], James R. Zimbelman [d], Christopher W. Hamilton [e], W. Brent Garry [a], Larry S. Crumpler [f], David A. Williams [g]

[a] NASA Goddard Space Flight Center, Planetary Geology, Geophysics and Geochemistry Laboratory, Greenbelt, MD 20771, USA
[b] Hawaiian Volcano Observatory, U.S. Geological Survey, Hawaii National Park, HI 96718, USA
[c] Franklin & Marshall College, Department of Earth and Environment, Lancaster, PA 17604, USA
[d] Center for Earth and Planetary Studies, Smithsonian Institution, National Air and Space Museum, Washington, D.C. 20560, USA
[e] University of Arizona, Lunar and Planetary Laboratory, Tucson, AZ 85721, USA
[f] New Mexico Museum of Natural History and Science, Albuquerque, NM 87104, USA
[g] Arizona State University, School of Earth and Space Exploration, Tempe, AZ 85287, USA

ARTICLE INFO

Article history:
Received 20 May 2016
Received in revised form 24 February 2017
Accepted 23 March 2017
Available online 29 March 2017

Keywords:
Lava flow emplacement
Inflation
Mars
Hawaii
Sinuous ridges
Morphology

ABSTRACT

The Tharsis Montes rift aprons are composed of outpourings of lava from chaotic terrains to the northeast and southwest flank of each volcano. Sinuous and branching channel networks that are present on the rift aprons suggest the possibility of fluvial processes in their development, or erosion by rapidly emplaced lavas, but the style of lava flow emplacement throughout rift apron development is not clearly understood. To better characterize the style of lava emplacement and role of fluvial processes in rift apron development, we conducted morphological mapping of the Pavonis Mons southwest rift apron and the eastern Tharsis plains using images from the High Resolution Imaging Science Experiment (HiRISE), Mars Orbiter Camera (MOC), Context Camera (CTX), Thermal Emission Imaging System (THEMIS), and High Resolution Stereo Camera (HRSC) along with the Mars Orbiter Laser Altimeter (MOLA) Precision Experiment Data Records (PEDRs) and gridded data. Our approach was to: (1) search for depositional fans at the slope break between the rift apron and adjacent low slope plains; (2) determine if there is evidence that previously formed deposits might have been buried by plains units; (3) characterize the Tharsis plains morphologies east of Pavonis Mons; and (4) assess their relationship to the rift apron units. We have not identified topographically significant depositional fans, nor did we observe evidence to suggest that plains units have buried older rift apron units. Flow features associated with the rift apron are observed to continue across the slope break onto the plains. In this area, the plains are composed of a variety of small fissures and low shield vents around which broad channel-fed and tube-fed flows have been identified. We also find broad, flat-topped plateaus and sinuous ridges mixed among the channels, tubes and vents. Flat-topped plateaus and sinuous ridges are morphologies that are analogous to those observed on the coastal plain of Hawai'i, where lava flows have advanced from the volcano's several degree flank onto the nearly zero degree coastal plain. When local volumetric flow rates are low, flow fronts tend to spread laterally and often thicken via endogenous growth, or inflation, of the sheet-like flow units. If flow advance is restricted by existing topography into narrow pathways, inflation can be focused into sinuous, elongate ridges. The presence of plateaus and ridges—emplaced from the rift zones, across the plains to the east of Pavonis Mons—and a lack of fan-like features, or evidence for their burial, are consistent with rift apron lavas crossing a slope break with low local volumetric flow rates that led to inflation of sheet-like and tube-fed lava flows.

1. Introduction

The Tharsis Volcanic Province of Mars is a broad volcanic rise that includes several large shield volcanoes, including the NE-trending chain of the Tharsis Montes, Arsia, Pavonis, and Ascraeus Mons (Fig. 1) (Carr et al., 1977; Greeley and Spudis, 1981; Mouginis-Mark et al., 1992; Hodges and Moore, 1994). These volcanoes have each experienced an episode of main flank development involving eruptions from the summit, followed by rifting to the northeast and southwest, to form extensive rift zones and deposits that are collectively known as the Tharsis Montes rift aprons (Fig. 2) (Carr et al., 1977; Crumpler et al., 2007). The rift aprons are thought to have largely involved lava emplacement from within the chasmata (chaotic terrains formed by collapse of the

* Corresponding author.
E-mail address: jacob.e.bleacher@nasa.gov (J.E. Bleacher).

http://dx.doi.org/10.1016/j.jvolgeores.2017.03.025
0377-0273/

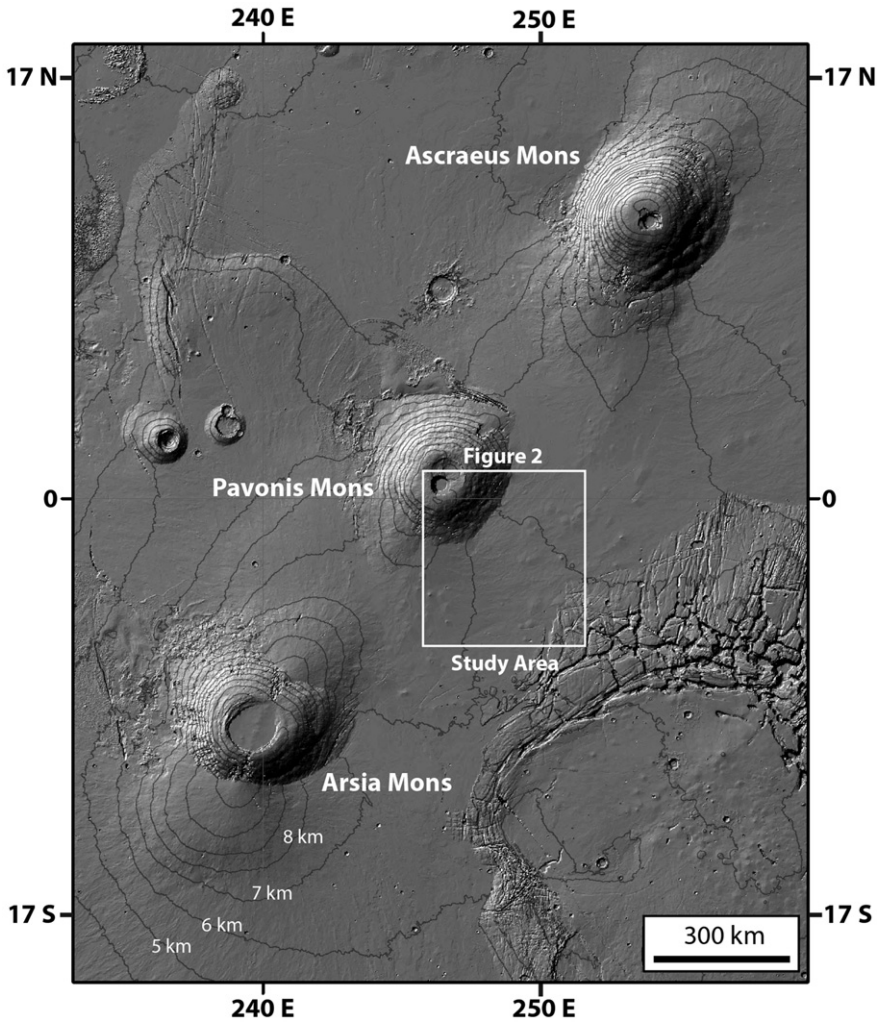

Fig. 1. MOLA shaded relief image of the Tharsis Montes. Each shield volcano displays a main flank and rift aprons to the NE and SW. The change from main flank to rift apron and vent field involves a decrease in slope from 4–6° to 1–3°. The rift apron and vent field flows extend out onto the regional Tharsis plains, where slopes decrease to <1°. The study area in Fig. 2 is shown in the white box. Contours shown in black are at a 1 km interval, and labeled to the South of Arsia Mons.

main flank) (Carr et al., 1977; Crumpler et al., 2007). Post-Viking era data have shown that rift apron development involved significant lava emplacement through rift zone-aligned groups of low shields and fissure vents (Plescia, 2004; Bleacher et al., 2007a; Bleacher et al., 2009). Some lava flows erupted during rift apron development are at least several hundred kilometers long (Garry et al., 2007) and extend across a topographic and slope boundary that transitions from the 1° to 3° slope of the rift aprons (Plescia, 2004; Bleacher et al., 2007a) to the nearly 0° slope of the Tharsis plains.

It is also proposed that development of the rift aprons might have involved the release of large volumes of water, subsequent fluvial erosion, and/or possible emplacement of mud deposits (Mouginis-Mark and Christensen, 2005; Murray et al., 2010). Murray et al. (2010) suggest that the rift aprons themselves might be composed primarily of mud flows instead of lava flows. The features that lead to this interpretation are complex channel networks, which are typically composed of single-stem non-leveed rilles that can also display sections of branching channels with terraced walls and islands. These features can be over 100 km in length and rarely display obvious lateral or distal margins. Bleacher et al. (2007a) conducted morphologic mapping of portions of the Tharsis Montes southwest rift aprons, and suggested these complex channels result from modification of existing surface units, which they called the channel network terrain (CNT). However, Bleacher et al. (2007a) did not present an interpretation of the mode of modification. Mouginis-Mark and Christensen (2005) and Murray et al. (2010) suggested that the source of this surface modification was erosion by overland flow of water (Fig. 3). However, no fluvial depositional features have been identified as would be expected if fluvial erosion cut channels 10 s to 100 s of kilometers long. Although a fluvial erosion interpretation is difficult to explain if no depositional fans are associated with the channels, it is possible that these features might have been buried by subsequent lava emplacement, if the plains flows are younger than the rift aprons (including any fluvial activity). This is possible as the abundant volcanic vents identified on the Tharsis plains (Plescia, 2004; Bleacher et al., 2007a, 2009; Keszthelyi et al., 2008; Baptista et al., 2008; Baratoux et al., 2009; Hauber et al., 2009, 2011; Wilson et al., 2009; Brož and Hauber, 2012; Richardson et al., 2013; Brož et al., 2014) could be comparatively young (Hauber et al., 2011) and could represent volcanic plains that are genetically unique from the rift apron flows. Regardless, active lava flows can also produce depositional fans at slope breaks as lava is debouched from channels onto the lower slope terrain (Carr and Greeley, 1980). Thus, the lack of depositional fans at this slope break would neither definitively support nor refute either hypothesis.

Numerous investigations have described morphologies and structures within the rift aprons (Plescia, 2004; Mouginis-Mark and Christensen, 2005; Garry et al., 2007; Bleacher et al., 2007a, b; Mouginis-Mark and Rowland, 2008; Bleacher et al., 2009; Murray et al., 2010), but only a few studies (e.g., Garry et al., 2007), focused on lava flows extending from the rift aprons onto the adjacent Tharsis

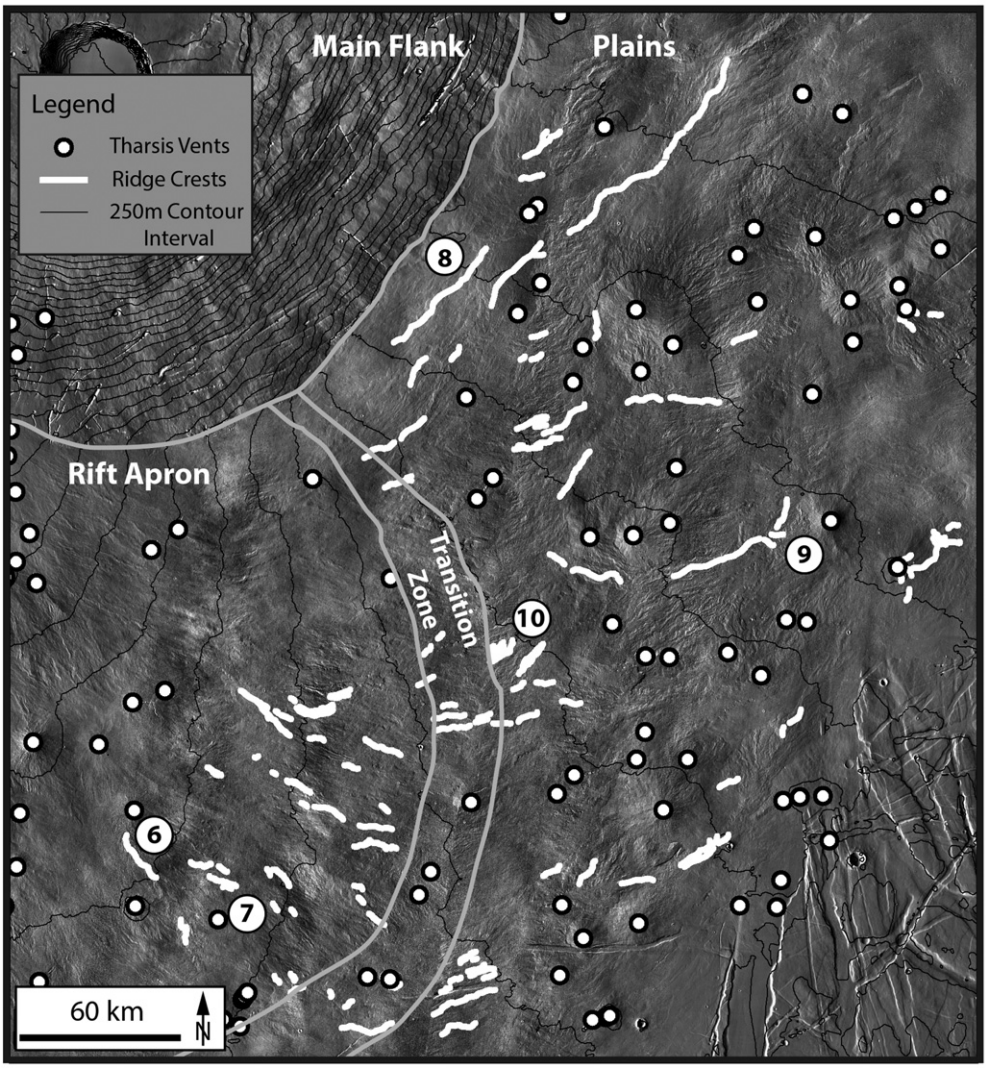

Fig. 2. This THEMIS Daytime IR mosaic (256 pixel/degree) shows the study area for the project, which is to the SE of the Pavonis Mons main flank. White circles mark volcano vents that are present both within the rift apron and across the Tharsis plains. White lines mark the crests of sinuous plains ridges that extend away from the Pavonis Mons rift apron, generally perpendicular to slope. Gray lines mark the boundaries between regions, including the main flank, rift apron and plains. The transition zone marks the area where ridge orientations change from NW–SE (rift apron) through W–E in the transition zone, to SW–NE in the plains. The locations of Figs. 6–10 are noted in this figure as numbers within a larger white circle.

plains units. Yet, understanding the geologic relationship between the apron and plains units is critical to constraining the origin of some apron features and possibly the aprons themselves. Furthermore, channel formation by erosive processes holds great implications for constraining the abundance and timing of aqueous processes on the surface of Mars. However, channels formed either by fluvial or volcanic processes can share many common features (Baker et al., 2015), and so it is critical to evaluate channel origin based not only on analysis of the channels in isolation, but also within their local and regional geologic context.

Our goal is to better characterize the style of lava emplacement and role of fluvial processes in rift apron development, including possible erosion by water or lava. Fluvial erosion would suggest storage and release of ground water whereas lava erosion could suggest high eruption and emplacement rates (Murray et al., 2010). To understand the style of lava emplacement in the rift aprons we use observations of lava flow morphologies to better constrain emplacement processes related to volcanic deposits. We present observations of the southwest rift apron of Pavonis Mons and the adjacent Tharsis plains to the east in an effort to understand the developmental history of the region (Fig. 2). Our approach is to (1) search for deposits at the slope break to assess their mode of origin, (2) determine if previously formed depositional features might have been buried by plains units, (3) characterize the Tharsis plains morphologies east of Pavonis Mons, and (4) assess their relationship to the rift apron units. Analyses of the rift aprons have not led to conclusive determinations of the role that water played in the evolution of the rift apron, and so we also examine the plains units to provide insight into the development of the rift apron units.

2. Background

The Tharsis region is covered by a pervasive dust deposit that masks the geochemistry of the underlying basaltic crust (Ruff and Christensen, 2002), and studies of lava flow chemistry from spectral data are limited to the margins of the Tharsis rise (Lang et al., 2009; Ramsey and Crown, 2010; Giacomini et al., 2012; Crown and Ramsey, 2017). Lava flows in the Tharsis plains are estimated to have been formed by large eruptions with discharge rates of 10^2–10^5 m^3 s^{-1} over a time scale of years to decades and are suggested to generally be basaltic in composition (e.g., Zimbelman, 1998; Warner and Gregg, 2009; Garry et al., 2007; Hiesinger et al., 2007; Glaze and Baloga, 2006, Glaze et al., 2009; Baloga and Glaze, 2008). Lava flows can also be considered with respect to morphology throughout a flow field to provide insights into emplacement conditions. For instance, Peitersen and Crown (1999, 2000)

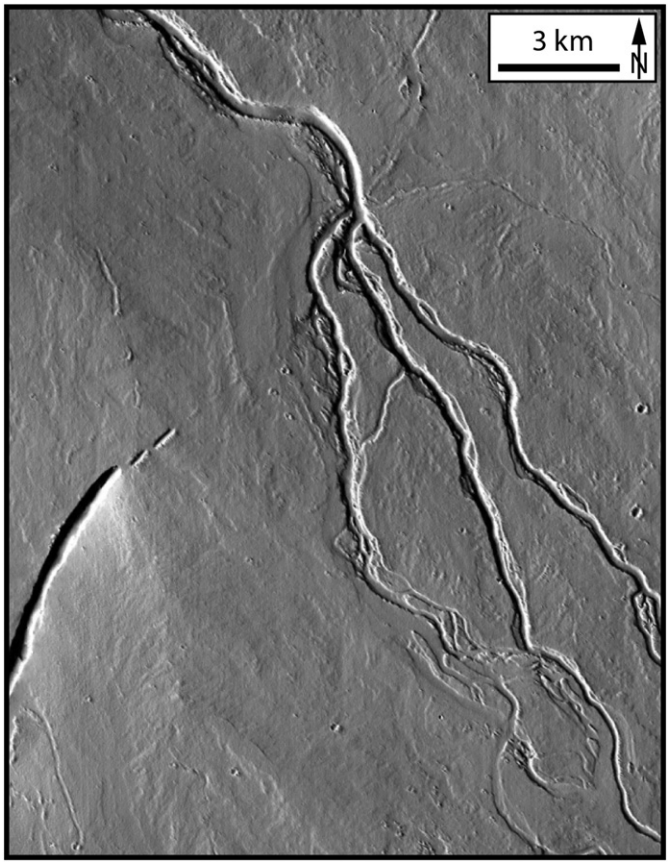

Fig. 3. CTX image CTX P08_004174_1862_XI_06N105W showing branching channel networks on the Ascraeus Mons SW rift apron (image center located at 6.4° N and 254.58° E). These channel networks are characterized by branching channel segments, channel terraces and islands and a lack of notable channel levees or lobate flow margins as are often seen associated with lava channels. These lines of evidence have led to the suggestion that this channel network, and similar others, are the result of erosion due to overland flow of either water or lava (Murray et al., 2010).

examined terrestrial and Martian lava flow morphologies as a function of distance from the vent (proximal, medial, and distal) providing a basis for subdividing flows and interpreting different morphologies within one flow field. Recently, Keszthelyi (2013) proposed a facies model for mafic lava flows to help provide insight into eruption duration and effusion rate that could also be applied to Mars. In this model, flow fields are divided into a near-vent, transport, and flow front facies, each of which is further divided between early-, middle-, and late-stages of development. Although much terrestrial research is focused on eruption conditions at a vent and the style of advance at a flow front, a significant surface area of our Martian study region comprises the transport facies of Keszthelyi (2013). Therefore, it is instructive to explore the development of transport pathways and structures within basaltic lava flow fields, and how these pathways evolve over higher (flank slope > 1°) and lower (plains slope < 1°) inclination terrains in Hawai'i as an analog for Mars.

It is generally considered that the effusion rate of an eruption is the largest control on the potential length of its related lava flows (Walker, 1973). However, the style of lava flow emplacement is related to many factors, of which the transport structure (open lava channel or insulated lava tube) (Malin, 1980) and local volumetric flow rate has a strong influence (Rowland and Walker, 1990). Although volumetric flow rate is largely controlled by the eruption rate, local conditions such as slope can also impose a strong effect. As such, the Hawaiian volcanoes and the Tharsis Montes, which both display main flanks (and rift aprons on Mars) with slopes >1° and plains units where slopes are much <1° serve as reasonable analogs to one another with respect to lava flow development that can be useful for interpreting observations of Martian lava flows. One factor to consider when studying transport pathways is the style of insulation; for instance, how much of the flow is partitioned into lava tubes versus exposed surface pathways or channels (Wentworth and Macdonald, 1953; Malin, 1980; Holcomb, 1987; Greeley, 1987; Mark and Moore, 1987; Moore and Mark, 1992; Calvari and Pinkerton, 1998, 1999; Rowland and Garbeil, 2000; Bleacher and Greeley, 2008; Harris and Rowland, 2009; Koeppen et al., 2013). Additionally, the morphology of a pathway will evolve based on the degree to which the lava within the pathway is flowing at full or decreased capacity as well as the style of lava insulation (Kauahikaua et al., 1998; Bailey et al., 2006; Harris and Rowland, 2009).

2.1. Hawaiian volcano flanks

During Hawaiian eruptions, two types of lava distribution pathways tend to form—open lava channels and closed (or nearly closed) lava tubes (Wentworth and Macdonald, 1953). Wentworth and Macdonald (1953) and Macdonald (1956) noted that channels quickly form within near-vent sheets of lava, due to velocity gradients between faster moving lava in the thickest, central sections of a flow and slower moving, thinner lava near the flow's margins (Hulme, 1974). Faster moving pathways within near vent sheets develop into channels as levees are initially constructed by lateral displacement of cooled crustal material. Eventually 'a'ā rubble at the flow front contributes to levee growth, which can also be enhanced by pāhoehoe overflows (Wolfe, 1988; Heliker and Mattox, 2003; Kauahikaua et al., 2003). Spatter, spillover, and breaching of the levees can produce small distributary flow lobes adjacent to the main channel, or can develop into a new primary channel branch, thereby producing a channel-fed flow field (Kilburn, 2000). As the flow cools or the eruption ends the channel can drain leaving an empty, leveed channel up to a few meters in height (Fig. 4). Drained channels tend to be rectangular in cross-section (Kauahikaua et al., 2003).

Lava tubes are also important for transporting lava from the vent to flow fronts, especially in pāhoehoe flows, an observation that has been confirmed repeatedly as eruptions locations have changed in Hawai'i (Wentworth and Macdonald, 1953; Macdonald, 1956; Holcomb, 1987; Greeley, 1987; Wolfe, 1988; Heliker and Mattox, 2003; Kauahikaua et al., 2003). Unlike open channels, mature tubes are tunnels enclosed by solidified lava and can be considered surface extensions of the conduit (Greeley, 1987). Wentworth and Macdonald (1953) indicated that lava tubes form through two dominant processes including the roofing over of active lava channels, and progressive advancement and connection between lobate toes at the flow front, eventually forming dominant pathways or tubes. Tubes that form by roofing over of a channel tend to do so by the (1) growth of rooted crusts, (2) accretion of new lava onto levees, thereby building an arch, and/or (3) welding together of floating crustal plates within the channel (Greeley, 1971, 1972, 1987; Swanson, 1973; Peterson and Swanson, 1974; Peterson et al., 1994; Hon et al., 1994; Calvari and Pinkerton, 1998, 1999). Tubes act to insulate the liquid lava, with measured temperature decreases of <1 °C/km traveled (Swanson, 1973; Helz and Thornber, 1987; Helz et al., 1993; Keszthelyi, 1995; Kauahikaua et al., 1998; Witter and Harris, 2007), which is far less than measured along active, open lava channels that lose heat more easily (Cashman et al., 1999; Harris et al., 2007; Harris and Rowland, 2009). The insulating nature of tubes enables lava to flow to longer distances than if it were emplaced through an open channel. The formation of lava tubes or channels has been shown to relate to volcano flank slopes with higher average flank slopes linked to lower abundances of longer lava tube-fed flows (Mark and Moore, 1987; Moore and Mark, 1992; Rowland and Garbeil, 2000; Bleacher and Greeley, 2008).

Tubes located on the flanks of Hawaiian shield volcanoes where slopes are >1° typically form via roofing over of active lava channels, although some do form within sheet flows (Kauahikaua et al., 1998). Tubes that evolve from open channels tend to form broad ridges and

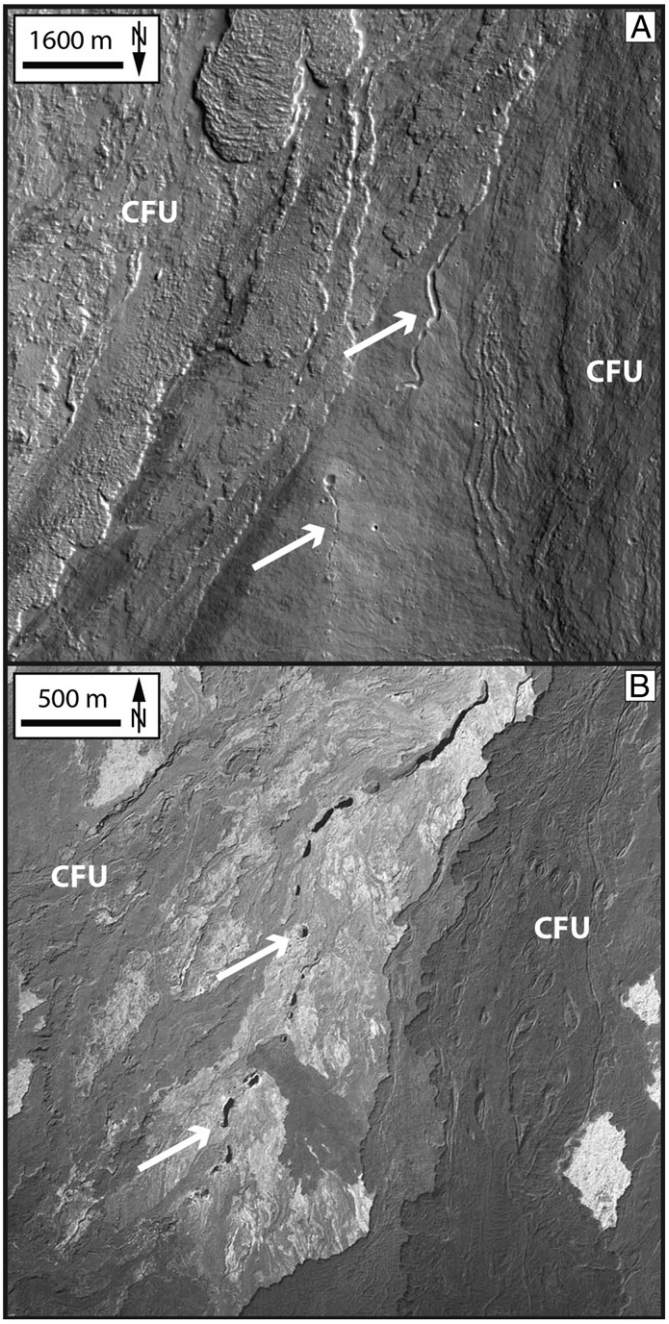

Fig. 4. A comparison of a tube-fed unit and adjacent channel-fed units (CFU) as mapped by Bleacher et al., (2007a, b) on Olympus Mons and the Tharsis Montes. Panel A shows the Olympus Mons northern flank and Panel B shows the Pōhue Bay lava tube on Hawaii. Note that north is to the bottom of Panel A to match the orientation of pits and flow direction in both panels for ease of comparison Both features are located on the flank of a large shield volcano across slopes of several degrees. In both cases the tube-fed flow shows open roof segments or skylights axial to a ridge (white arrows), which display a relatively smooth surface. The topography of the tube-fed unit controlled the flow direction of flows in the younger channel-fed units that have embayed the tube's lateral margins. Panel A shows CTX image B12_014420_2022_XN_22N132W. The Pōhue Bay lava tube image in Panel B comes from image EKL-9CC-188 acquired on January 22, 1965 by the USDA Farm Service Agency, and this image is in the public domain.

do not regularly flow at full capacity (Kauahikaua et al., 1998). Unsteady volumetric flow rates that sometimes exceed the volume of the tube, either within tubes that form via roofed channels or tubes formed within a sheet, can lead to disruption of the overlying crust of an established lava tube. This process can lead to the production of rootless shields that form by the repeated stacking of short breakout lava flows at the site of disruption (Kauahikaua et al., 2003; Patrick and Orr, 2011), or localized disruption of the tube roof creating raised-rim features called shatter rings (Orr, 2010). Rootless shields can also form progressively as a tube-fed flow advances. In both cases, rootless shields can store a substantial volume of lava. This lava can be released abruptly if the flank of a shield fails, thereby producing short-lived increases in local volumetric flow rate. This process can emplace channelized ʻaʻā flows within a flow field dominated by tube-fed pāhoehoe (Patrick and Orr, 2011). The development of rootless shields over lava tubes in Hawaiʻi has produced broad ridges up to 20 m in height and >1 km across. An important observation is that a single eruption can produce a range of structures and morphologies over the length of the associated lava flow due to changes in eruption conditions at the vent, variations in local conditions, and influences from pre-flow topography. Variance in morphology and structures across a flow field is likely to be higher or potentially more pronounced the longer-lived an eruption is/was.

2.2. Tharsis volcano flanks and rift aprons

The main flanks and rift aprons of Tharsis shield volcanoes display similar morphologies to terrestrial shield volcanoes (Holcomb, 1987). Long, ribbon-like channelized flows are easily observed across Martian volcanoes (e.g., Morris and Tanaka, 1994). These flows often appear to be boxy in cross-section with well-developed levee systems (Fig. 4).

Lava tube-fed flow fields have also been mapped on the flanks of larger Tharsis shield volcanoes (Fig. 4) (Pupysheva et al., 2006; Bleacher et al., 2007a,b). They form broad ridges up to 100-m-high and several kilometers across (hereafter called flank ridges). Sinuous rilles or chains of rimless pits are typically located along the axis of broad ridges. Many rilles or pits are sources for small overbank flows that together coalesce to define a broad ridge. Tube-fed flow fields also display significant breakouts, known as fans (Carr et al., 1977; Morris and Tanaka, 1994; Mouginis-Mark and Christensen, 2005; Bleacher et al., 2007a). Lava fans are topographic features that also rise >100 m above the adjacent flank. These features decrease in local relief with distance from the breakout until grading into the flank flows. Although some fans could be eruption sites that are related to rift zone activity (Mouginis-Mark and Christensen, 2005) or magma migration along fault zones within the shield volcanoes (Morris and Tanaka, 1994), they are typically associated with upslope tube-fed flows that trend into the fan's apex. This relationship led Bleacher et al. (2007a) to conclude that they are most likely analogous to rootless shields, which are observed to form over some Hawaiian lava tubes (Patrick and Orr, 2011). Many of these fan features are found at locations where the pre-flow surface slope decreases (Fig. 5). Thus, these fan deposits on the flanks of Martian shield volcanoes, in some cases, might represent the type of lava deposit that can form when lava flows encounter breaks in slope.

In summary, the morphologies that are produced from a given eruption, whether on Earth or Mars, generally differ between the low slope plains and the shield's higher slope flanks. Flows on the flanks generally form leveed lava channels with a rectangular cross sectional appearance. If the eruption, or undisturbed eruptive episode, is long-lived, the channels can develop a roof, thereby forming a lava tube. Flank tubes generally do not flow at full capacity continuously, and the decoupling of the crust from the liquid core does not enable roof inflation. However, increases in lava flux through the tube can lead to disruption of the roof and the development of a rootless shield or series of shields. In this way, flank tube systems can develop broad ridges with chains of pits (or skylights, if active) and rootless shield vents aligned along the axis. These broad ridges or tube-fed flows are interspersed with lava channels across the main flank.

3. Methods

The main questions that motivated this project were: (1) What is the nature of the boundary between the Tharsis Montes rift aprons and the Tharsis plains; and (2) how are flow features in the two regions related?

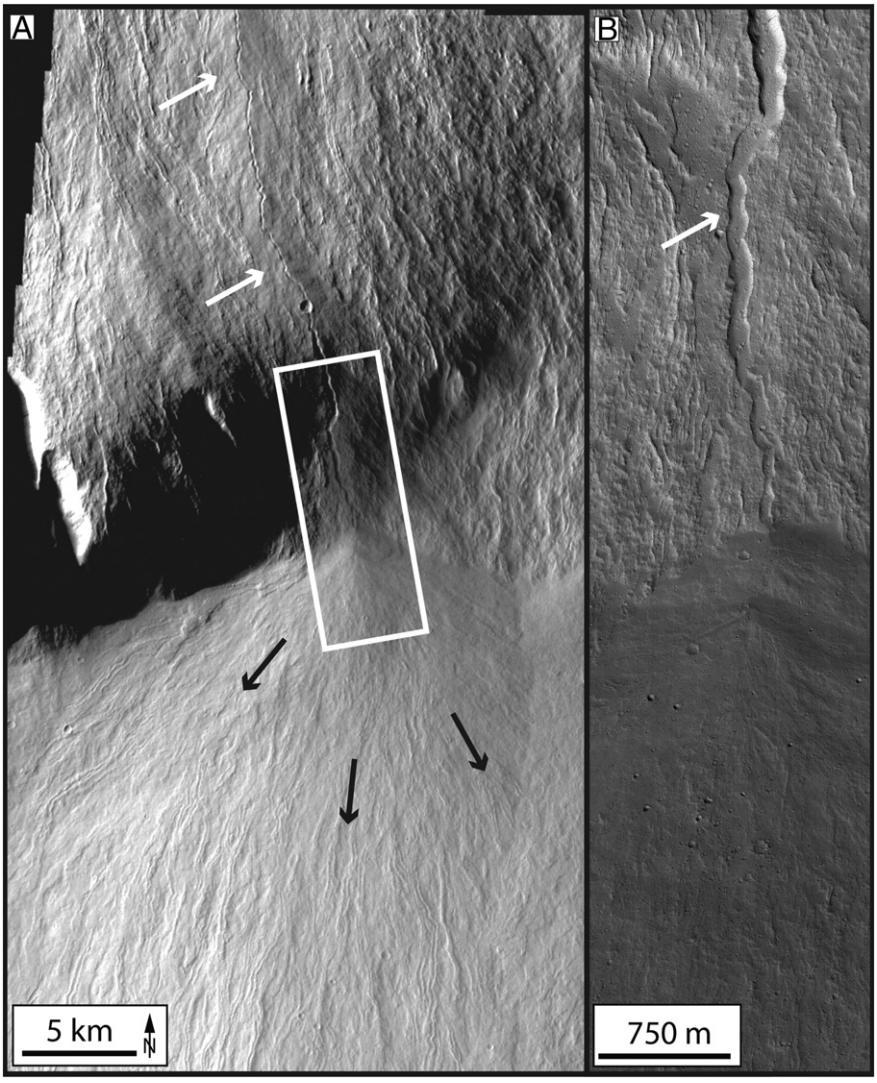

Fig. 5. A tube-fed flow located on the southern flank of Olympus Mons trends across a major break in slope from high to low. Panel A shows THEMIS a visible image mosaic including V12836015 and V14059010. The inset box in Panel A corresponds to Panel B, which shows MOC image S08-01421. Here the tube-fed flow developed into a lava fan as the flow pathway structure (tube, shown by white arrows in both panels) was disrupted, resulting in a large number of smaller channel-fed breakouts that flowed away from the fan's apex, or disruption point. All trace of the tube structure is lost once the transition occurs from a tube-fed flow to a lava fan dominated by lava small channels.

Although structures that typically serve as lava flow pathways are easily recognized on the flank and rift apron of Pavonis Mons, such as channels and tubes, sinuous and sometimes branching channel networks are of a less obvious origin. If these features formed due to erosion in the rift aprons, then depositional fans should be present at the slope break. If such deposits cannot be found, then two conclusions can be reached: either erosion is not the cause of the extensive branching channel networks located within the rift aprons, or all depositional fans have been buried by the younger deposits that compose the plains. Thus, the goal of this project was to map the slope break and search for fans or depositional fans and, if not found, to assess the nature of the contact at the slope break and the characteristics of the plains units as related to the rift apron units. The study region covers an area to the south and east of the Pavonis Mons main flank between 1° and −7° latitude and 247°E and 254°E longitude. This region includes portions of the Pavonis Mons SW rift apron, and the eastern Tharsis plains covering an area of ~ 206,600 km^2.

A project of this nature is only possible due to the successful data collection by multiple post-Viking orbiter missions at Mars. Integration of image data sets from these missions enables generally uniform coverage across the study area (Fig. 2). The acquisition of CTX (Malin et al., 2007), THEMIS (Christensen et al., 2004), and HRSC (Neukum et al., 2004) images has provided nearly complete visible image coverage of this study area at resolutions between 6 and 25 m/pixel. Although not providing region-wide coverage, higher resolution images from MOC (Malin et al., 1992) and HiRISE (McEwen et al., 2007) were used to enhance mapping interpretations. We have geo-referenced relevant images from these cameras to the THEMIS infrared daytime mosaic at 512 pixels/degree (~100 m/pixel) (Christensen et al., 2004) and the 128 pixels/degree (~460 m/pixel) MOLA gridded dataset (Smith et al., 2003). Maps were originally compiled using ArcGIS 9.3 by ESRI. Subsequent mapping was conducted using a combination of ArcGIS 9.3 through 10.3.

Morphologic mapping was conducted across the study region to identify flow boundaries and margins to assess what flow unit types are linked throughout the rift apron and across the plains. The goal was to link flow units of the rift aprons with their terminal margin and to assess if the terminal margin represents the natural end of the flow or is related to burial by a younger unit. For units that extend beyond the slope break the mapping was intended to determine if and how flow unit morphology changes with decreased slope. Fig. 2 shows the location of plains ridges as mapped within this project, and the location of plains volcanoes as mapped in the Catalog of Tharsis Province Small Volcanic Vents (Bleacher et al., 2009; Richardson et al., 2013).

Data related to the relief of a feature is based upon analysis of the MOLA PEDRs. Often, features were broad enough to be identified within the MOLA gridded data product as well. For smaller features, relief information obtained from the PEDR data was supplemented using shadow measurements. These results are considered to be far less accurate but nonetheless provide a constraint on a feature's relief. The orientation and size of many of the ridges made difficult a robust assessment of ridge dimensions across a flow field or between flow fields.

4. Results

The rift aprons of the Tharsis Montes are spatially related to the shield volcano they are adjacent to, but are often discussed as unique volcanoes in their own right (Crumpler et al., 2007; Plescia, 2004) potentially resulting from completely unique eruption events unrelated to the formation of the main shields (Bleacher et al., 2007a; Xiao and Wang, 2009; Murray et al., 2010). Because the physical makeup of the rift apron flows is questioned in the literature, while the main flank flows are not, we refer to main flank flows as "lava flows" and rift apron units as just "flows". Rift apron-sourced flows are younger than the main flank lava flows and consistently embay the base of the shield's main flanks indicating a time step between flank formation and rift zone apron development (Crumpler et al., 2007; Plescia, 2004; Bleacher et al., 2007; Xiao and Wang, 2009; Murray et al., 2010). Crater counts are consistent with these superposition relationships as main flank flows are suggested to display eruptions over a significant amount of time, but are as young as several hundred millions of years old (Werner, 2009) whereas rift apron units and small volcanic vents in the rift aprons are suggested to be as young as ~100 Ma (Werner, 2009) or younger (Hauber et al., 2013). The rift apron in part comprises units that are fairly similar in morphology to the main flanks of the Tharsis Montes and other Tharsis shield volcanoes, including a combination of broad, leveed channels and broad ridges that can stand up to 100 m above the adjacent terrain, which are inferred here to be lava channel-fed and lava tube-fed flows. Unlike the main flank of Pavonis Mons, the rift apron, as well as the plains east of it, display numerous low shields and fissure vents. Additionally, sinuous and sometimes branching channel networks are observed in the rift apron, but are not seen on the main flanks. These features are typically found within smooth units that do not display thick flow margins or channel levees but do possess islands and channel terraces. The dissimilarity between these features and traditional lava channel morphologies led Murray et al. (2010) to conclude that they must have formed as a result of erosion of the existing terrain by flowing water.

The relationship between the Pavonis Mons rift apron and the plains to the east is not as clear as the relationship between the rift apron and main flank. The boundary between the apron and the plains corresponds with a break in slope from the 1–3° rift apron to the 0–1° plains, without displaying a clear contact between units of different morphology or age. The boundary is better described as a transition zone (Fig. 2) sometimes with a gradual change over several 10 s of kilometers. Slopes are taken from the reports of Plescia (2004) and Bleacher et al. (2007a). In this study the MOLA gridded data product was used to derive a slope map at the scale of ~460 m/pixel. Rift apron flows in the study area typically trend south to southeast, but upon encountering the transition zone, flow orientations realign to east before taking on a northeast orientation on the plains (Fig. 6). At the slope break between the two terrains we do not identify any consistent embayment relationship from plains units. This observation is in agreement with the results of Garry et al. (2007), who identified a long lava flow that originates in the southwest rift apron of Ascraeus Mons and extends onto the plains without evidence of burial by a younger plains unit. Where it appears that plains units have buried rift apron units, the embayment relationship results from rift apron flows that cross the slope break to the south and realigned to flow to the northeast and bury older rift apron flows. No clear evidence exists for a true "plains unit" composed only of flows erupted from sources in the plains that consistently bury rift apron units. The transition across the slope break from the rift apron to the plains is accompanied by changes in flow field morphology. Along the rift apron's eastern slope break we do not identify any depositional fans. Flow fields typically become wider, taking on a smooth to muted appearance, sometimes obscuring channel and tube-related features near the contact. Within several kilometers from the slope break into the plains recognizable flow structures are once again observed.

In the plains, leveed channels and broad tube-related ridges are present that are comparable in both morphology and size to those observed on the rift apron and main shield flank and are again inferred to represent channel-fed and tube-fed lava flows. The sinuous and branching channel networks are not observed. Instead, sinuous plains ridges that are kilometers to several 10 s of kilometers in length, but as long as 100 km, some with distributary branching patterns are present. Sinuous plains ridges are identified in the distal margins of the rift apron where slopes approach 1°, across the transition zone and are routinely observed throughout the plains (Figs. 2 and 10). These sinuous plains ridges (Fig. 6) are distinctly different from the broad ridges (lava tube-fed flows) described earlier (Fig. 4). Sinuous plains ridges can be subdivided into a narrow ridge and in some cases a lower broad rise. The narrow ridges are tens to hundreds of meters across and estimated to be up to 10 m in height (based on shadow measurements and, where possible, MOLA PEDR data). In some instances narrow ridges are located along the axes of topographically lower, broad rises that can be up to several kilometers across, while in other instances the narrow ridges are present within an otherwise featureless plain (Fig. 7). Some sinuous plains ridges (including a narrow ridge and lower broad rise) can rise 40 m above the adjacent plains, as measured using MOLA PEDR data. Due to the small size of ridges and orientations that are not conducive to elevation determinations from either shadow measurements or MOLA PEDR data a presentation of consistent measurements between ridges or even along a single ridge is not possible. However, the purpose of this effort was to attempt to place some constraints on ridge and plateau dimensions. Sinuous plains ridges tend to follow the regional slope and often weave between existing high topography such as shields or thick flow features. Thus, whereas the broad ridges (tube-fed flows) seen on the main flank, rift apron and elsewhere in the plains are up to 100 m in height, the sinuous plains ridges are roughly half as thick and are generally topped by a narrow ridge rather than a sinuous series of depressions and pits.

The sinuous plains ridges display morphologic variability (Fig. 8) across the plains, and sometimes within a single flow. They appear to vary in height and width, sometimes disappearing from view, but reappearing short distances away. Small, generally smooth-textured, lobes of lava hundreds of meters to kilometers in length can be seen to have originated at the base of the narrow ridge component of sinuous plains ridges. Where these lobes are common and stacked they compose the lower broad rise component of a sinuous plains ridge similar to the way in which small breakout lobes of lava stack to atop the broad (tube-fed) ridges. Narrow ridges can display a single crest or double crest. Double-crested walls also sometimes display another central ridge along the trough between the crests, or they can display flat floored troughs. In some areas the flat floored troughs are quite wide, sometimes extending several tens of meters across the top of the narrow ridge.

Sinuous plains ridges sometimes terminate as broad, flat-topped plateaus with heights 40 m above the surrounding plains as measured using MOLA PEDR data (Fig. 9). The margins of these plateaus are often irregular and lobate in map view, sometimes stepping down to lower topography lobes or terraces that are similar to the lobes associated with the lower broad rise of a sinuous plains ridge. The interiors of the plateaus often include numerous circular to irregularly shaped depressions that appear to be as deep as or shallower than the thickness of the plateau. Often the plateaus form in locations where the ridges trend towards and terminate against a topographic obstacle, such as a low shield or thick lava channel or tube-fed flow (Fig. 9).

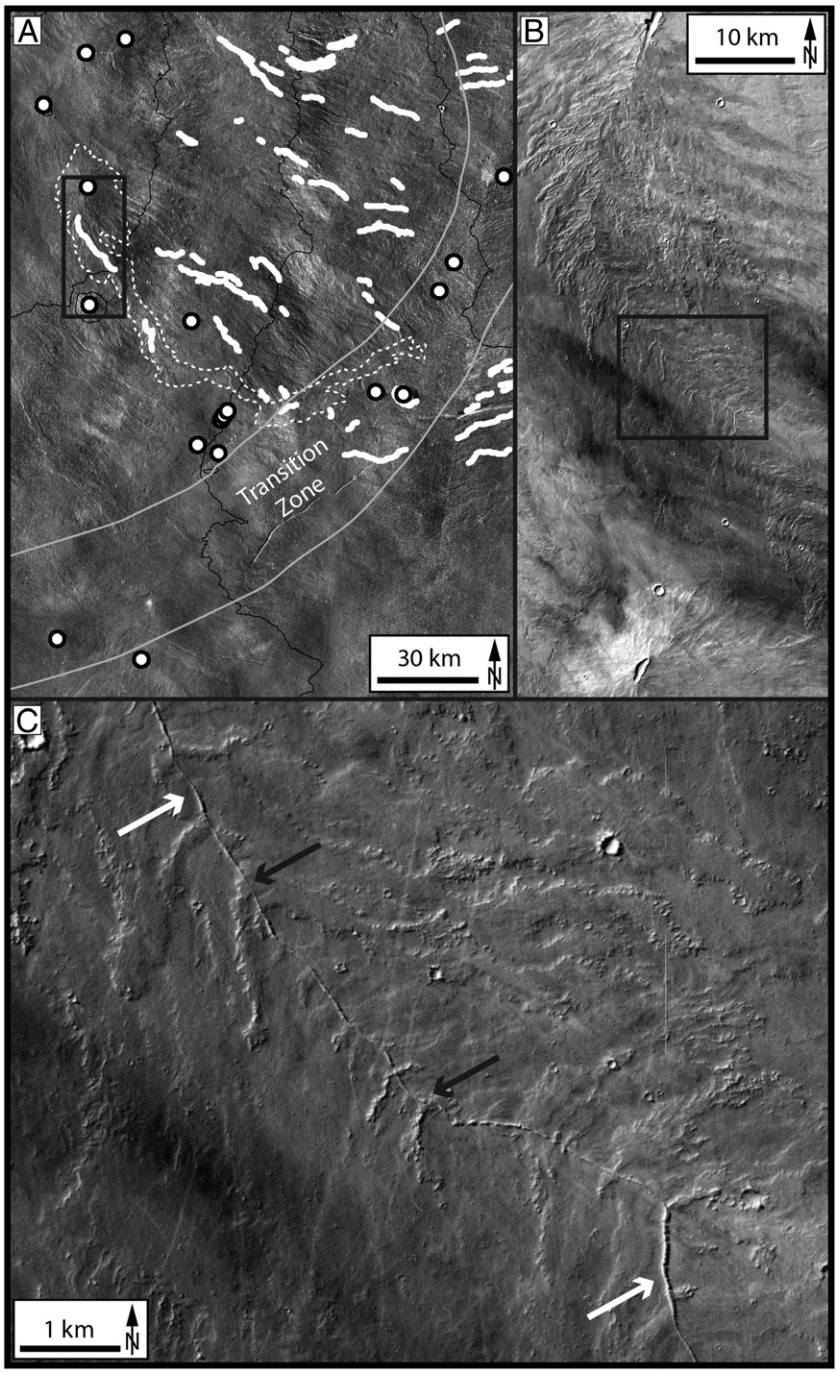

Fig. 6. Panel A shows a section of the THEMIS 256 pixel/degree mosaic with white circles marking volcano vents and solid white lines marking sinuous ridges (as shown in Fig. 2). The dashed white line marks the margin of a single lava flow field. The inset box in Panel A matches with Panel B and shows the vent and proximal section of the lava flow outlined in Panel A. This flow field displays several sections with visible ridges and also shows a change in flow direction from approximately southeast to east and northeast as it crosses into the transition zone. Panel B is taken from CTX image P20_008934_1756_XI_04S112W. The inset box in Panel B corresponds to Panel C, which comes from the same CTX image and shows a more detailed view of a flow section displaying ridge formation (white arrows) around which small breakout lobes can be observed (black arrows). Many Tharsis plains ridges do not display a clear source as their proximal sections are buried by younger lava flows.

Sinuous plains ridges are distributed across the plains, but their sources are indeterminable due to burial by younger lava flows. However, some examples exist where a sinuous plains ridge can be traced back to a low shield. Fig. 6 shows a low shield vent that is located near the slope break between the rift apron and the plains. This low shield is the youngest feature in the area and fed a 100-km-long lava flow. As this flow transitions off of the low shield's flank onto the regional plains, the lava flow develops a sinuous plains ridge up to 30 m in height. Many breakouts are clearly visible extending from the base of this feature's narrow ridge. Similar evidence is visible in the plains east of the Pavonis Mons where a low shield is seen in HiRISE Camera image ESP_027289_1790 to have emplaced a much shorter sinuous plains ridge (see Fig. 8 of Orr et al. (2015)).

In this study, we identified 163 unique sinuous plains ridge segments within the study area using CTX and THEMIS. However, the presence of sinuous plains ridges in higher resolution data (Orr et al., 2015), which do not provide complete coverage of the study area suggests that this number is but a subset of the total population. Conversely, some unique segments might be part of the same lava flow. Thus, the abundance of sinuous plains ridges discussed here is merely meant to

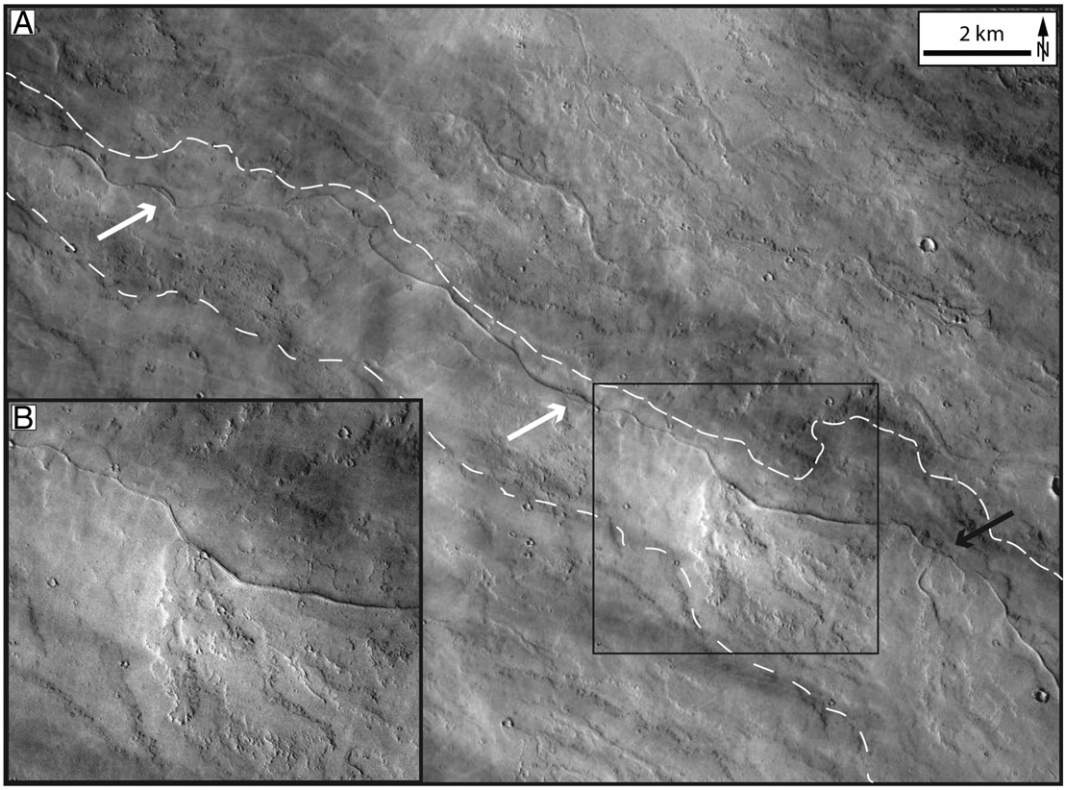

Fig. 7. CTX image B10_013615_1758_XI_04S111W shows a typical Tharsis sinuous plains ridge trending from the top left (NW) to bottom right (SE). The ridge is composed of two parts, a lower broad rise (marked by the dashed white lines) and a sinuous, narrow ridge located on the axis of the rise. The height of the wall-like structure appears to vary sometimes becoming indistinguishable. Often small lobes appear to source from the base of the wall-like structure at or near sharp bends as is shown in Panel B, which corresponds to the inset box in Panel A. These small lobes stack upon each other and together form the underlying broad ridge. Sometimes the wall-like structure appears to produce a double-crested narrow ridge (white arrows) and shows evidence of forming a branching distributary network (black arrow).

demonstrate that these features are common within the Tharsis plains East of Pavonis Mons.

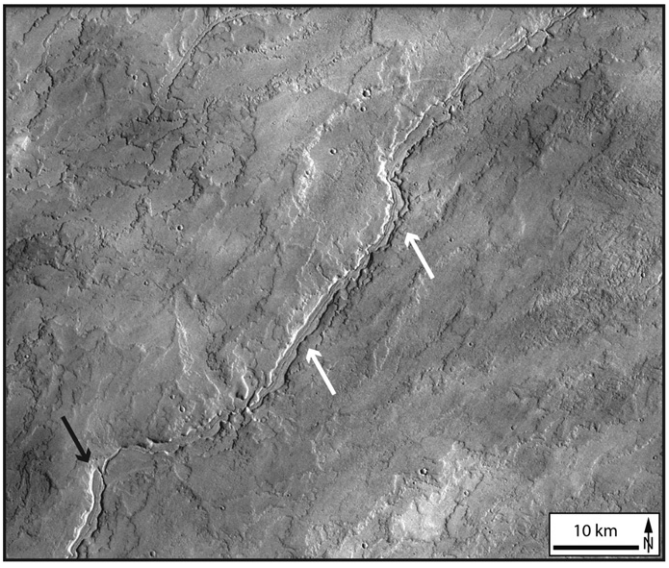

Fig. 8. CTX image B06_011848_1790_XN_01S110W shows a sinuous plains ridge with a complex wall-like structure trending from the bottom left (SW) to the top right (NE) of the image. This example shows double-crested narrow ridges, sometimes with broad flat to slightly depressed tops. Some sections of the ridge display a second narrow ridge within the depressed portion of the broader double crested narrow ridge (white arrows) as well as terraced margins. To the lower left (SW) the ridge appears to have a pond-like structure and might represent a feature that is transitional between an inflated roof and a perched lava channel (black arrow).

In summary, the boundary between the Pavonis Mons rift apron and eastern Tharsis plains is a topographic boundary between the higher elevation, more steeply sloping rift apron and the lower elevation, more gently sloping plains. No consistent superposition between the two terrains is observed. Depositional fans are not present and do not appear to have been buried by plains flows, because flows from the apron can be traced across the slope break beyond which they can be seen to decrease in thickness and broaden. Lacking in the plains are the sinuous and branching, non-leveed channel networks that are observed in the rift apron flows. Characteristic of and concentrated in the plains with respect to the rift apron are sinuous plains ridges and broad plateaus that are interspersed with other plains units, including low shields, channel-fed and tube-fed lava flows. The morphologies described here are comparable to those described by Crown and Ramsey (2017) for the Tharsis plains to the southwest of Arsia Mons and in northeast Daedalia Planum. Crown and Ramsey (2017) identified sinuous ridges and plateaus that were associated with a relatively thin, low viscosity flow type; these features were interpreted to be segments of lava transport pathways that also included narrow channels upstream. The lower broad rises associated with sinuous ridges as described near Pavonis Mons were not evident in their study area.

5. Discussion

The rift aprons are traditionally thought to represent emplacement of lava flows (Carr et al., 1977; Crumpler et al., 2007; Plescia, 2004; Bleacher et al., 2007a, 2009). However, branching channel networks on the rift aprons have led to the suggestion that erosion has occurred (Mouginis-Mark and Christensen, 2005; Bleacher et al., 2007a; Murray et al., 2010). The style and extent of the purported erosion has also led to the suggestion that the rift aprons are composed of loosely

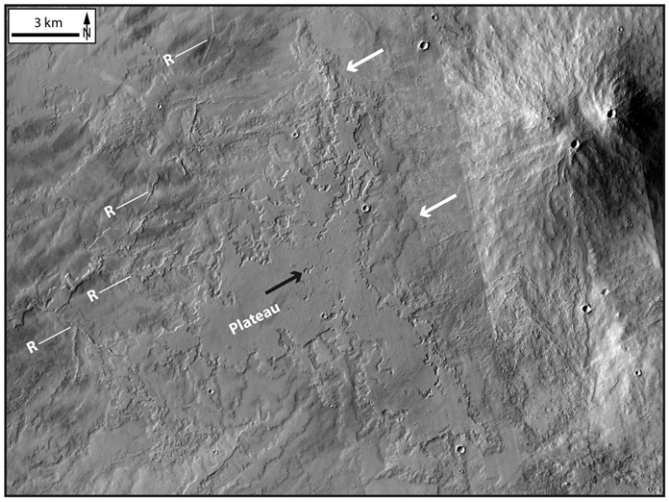

Fig. 9. Image mosaic combining CTX image B01_009870_1778_XI_02S108W (left) and P02_001906_1776_XI_02S108W (right) showing a Tharsis sinuous plains ridge that trends from lower left (SW) towards the upper right (NE). However, this flow encountered a topographic obstacle in the form of a low shield volcano. This geometry produces a slope break from low to high and inhibited the lateral advance of the flow. Here the morphology changes abruptly from a series of ridges to a broad, flat-topped plateau. Plateaus often include numerous irregularly shaped depressions (black arrow) likely analogous to lava rise inflation pits (Walker, 1991, 2009). The margins of the plateau is often irregular and lobate in map view, sometimes transitioning to a number of lower topography lobes or terraces that are similar to the lobes associated with ridges (white arrows). A detailed map of the same lava flow is presented by Healy and Zimbelman (2016). The sinuous plains ridge (marked by an R and thin white line) can be difficult to discern this scale. As the flow inflated to produce a plateau that no longer advanced to the northeast, breakouts to the north established new narrow pathways (R) that advanced in the topographic trough that was established between the high topography of older flows to the northwest and its own inflated flow front and the adjacent low shield.

consolidated material rather than competent lava flows. This has led to an interpretation that the rift apron units are composed of mud flows (Murray et al., 2010) that were subsequently eroded by discharge of water along fissures (Mouginis-Mark and Christensen, 2005; Murray et al., 2010). Although the rift aprons display morphologies consistent with lava tube and lava channel formation (Bleacher et al., 2007a), it is nonetheless possible that the branching channel networks represent a mixed genesis involving both emplacement of lava flows and more easily eroded mud flows. These considerably different interpretations of rift apron development have strong implications on the timing, nature and volume of volatiles on the surface of Mars, including the development of aquifers high up on the flanks of shield volcanoes. Thus, the motivation for this project was to characterize the relationship between the Pavonis Mons southwest rift apron flows (Bleacher et al., 2007a) and the adjacent Tharsis plains units to the east in an attempt to better characterize the geologic development of the rift aprons.

The 1–3° slopes of the rift apron transition into the nearly flat terrain of the plains. The slope break that bounds these two terrains shows no evidence for the development of depositional fans. This boundary also lacks consistent superposition relations between units of the two terrains. Some rift apron flow units transition onto the lower slope surface and show evidence for widening of the flow and a change in orientation from NW–SE to SW–NE. Where burial of the NW–SE-trending rift apron flows by the SW–NE-trending plains flows is observed, those plains flows are of unknown origin or an extension of younger rift apron flows that cross into the low slope plains terrain and changed orientation. In other words, plains lavas to the east of Pavonis Mons do not appear to represent a different eruptive event from a different volcano, but are composed of the same materials that currently make up the surface of the rift apron. Thus, at least to the east of Pavonis Mons, the Tharsis plains were resurfaced by the same flows that produced the southwest rift apron. This is consistent with observations of rift apron flows at Ascraeus Mons that extend from within the southwest rift apron out onto the Tharsis plains to the west and north of the volcano (Garry et al., 2007). This observation is also consistent with the units of the rift apron and extensive plains to the southwest of Arsia Mons, where long, rugged lava flows with well-developed central channels and lateral levees are intermingled with extensive flows fed by lava tubes and small channel/sinuous ridge systems (Crown and Ramsey, 2017).

The makeup of the boundary between the rift apron and plains suggests that the units comprising the two are the same. Fluvial channels formed by the erosion and transport of material must deposit the material in some other location. Deposition of this material occurs when water is no longer capable of transporting the clastic load. This process of deposition tends to produce deltas (if deposited into a large body of water) or alluvial fans (if deposited sub-aerially). If a sedimentary deposit is not associated with a channel then the transported sediments must have been removed due to subsequent erosion or are buried. Lava flows that encounter a slope break can also produce fan-like deposits (Carr and Greeley, 1980) and similar features are seen elsewhere on Tharsis volcanoes where lava flows encounter a steep to shallow slope break (Morris and Tanaka, 1994; Bleacher et al., 2007b) (Fig. 5). Lava flow deposition into a fan-like deposit occurs in this manner because the slope break causes disruption of the flow and rapid cooling, which increases viscosity and stalls the lava advance. Subsequent lava is emplaced over this stalled front and slowly produces a fan-like build-up of cooled lava until a new pathway structure is established to transport lava beyond the slope break. Thus, a lack of fan deposits might be inconsistent with either interpretation for rift apron development.

The youngest flow units of the rift apron can be traced onto the plains. Thus, a characterization of flow emplacement on the plains provides insights into the origin of rift apron units. The flows that compose the plains also display evidence for lava channels and tube-fed flows. However, whereas the rift apron channels and tubes are interspersed with branching channel networks, the plains channels and tubes are interspersed with ridges and plateaus (Fig. 10). Ridges and plateaus are not always found in association with one another in the same flow. However, their fairly common association suggests that the two features, even when found separate from one another, share a common developmental history. The ongoing eruption at Kīlauea volcano, Hawai'i, provides insight into the development of ridges and plateaus where lava flows have advanced across steep to shallow slope breaks and where advancing lava flows are confined by topography.

Kīlauea's East Rift Zone eruption has been ongoing since 1981 and been dominated by effusion from the Pu'u 'Ō'ō vent (e.g., Heliker and Mattox, 2003, Orr et al., 2015). Lava flows from Pu'u 'Ō'ō that reach the coastal plain, where slopes drop below 1°, commonly spread laterally as a thin sheet from their tube or channel system and subsequently thicken via flow inflation (Walker, 1991, 2009; Mattox et al., 1993; Peterson et al., 1994; Hon et al., 1994; Self et al., 1998; Hoblitt et al., 2012; Hamilton et al., 2013). Unlike lava tubes on the steeper sloping flanks of the volcano that typically flow below full capacity once they have formed, resulting in a decoupling of the roof and liquid core of the flow (Kauahikaua et al., 1998), sheet flows tend to involve a broad liquid core that remains coupled with the overlying crust (Hon et al., 1994) for a longer period of time. At a given location within a flow field, sheet flows initially experience an inflationary phase that involves growth or thickening of the liquid core itself (Hon et al., 1994). This phase is followed by a period of core stabilization, during which lava passes through this portion of the sheet to the active flow front (Hon et al., 1994). At this point, sheet inflation is driven by cooling of the liquid core and accumulation of crystals along the bottom of the upper crust and, to a lesser extent, the top of the lower crust. The liquid core cannot be infinitely compressed, and so upward lifting of the crust, or inflation, must accommodate the volume change associated with addition of new crustal material. In this way, toe structures at the flow front that are 10 s of cm thick are lifted upwards above a relatively continuous liquid core across the flow field resulting in flow lobes that can reach several meters in thickness. Unless later

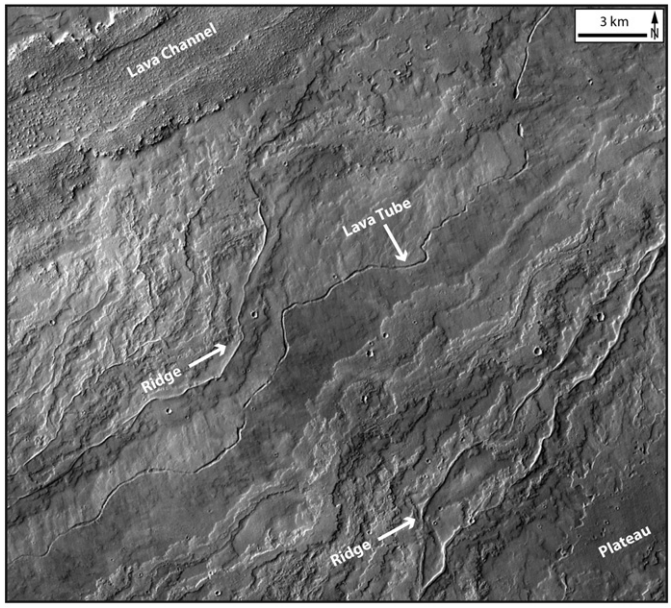

Fig. 10. CTX image G02_018929_1772_XN_02S110W showing an example of the primary morphologies that make up the Tharsis plains. Comparable to the higher slope flanks of the larger shield volcanoes, large channels are present as are tube-fed flows that appear as broad ridges along which the axes are marked by a sinuous trench or sinuous chain of pits. Interspersed between these volcanic features are features indicative of lava flow inflation, including volcanic ridges and plateaus. Inflation is often forced within lava flow emplacement where lateral advance of the flow is inhibited despite a continued supply of lava into the flow field. Inflation can be affected by obstacles as small as several meters and the older, channel- and tube-fed flow fields as well as small volcanoes provide ample opportunity to meet these conditions.

disrupted, these inflated surfaces preserve the original lava texture (Walker, 1991, 2009; Mattox et al., 1993; Peterson et al., 1994; Hon et al., 1994; Self et al., 1998; Hoblitt et al., 2012).

Continued seaward advancement beyond the slope break is slow, often taking weeks for the flow front margin to reach the coastline. However, once the flow front reaches the sea, lava within the fluid core of the sheet is preferentially focused into efficient pathways between the base of the scarp and the ocean outlet through the sheet. The development of a central pathway reduces the flow of new lava into the lateral margins of the sheet, which in turn reduces the rate of lateral spreading and leads to solidification of the core and stagnation of lateral advance and inflation. At this point a flow will be characterized by a well-developed tube within a broad sheet, or inflated plateau, comparable to proposed methods of forming tubes in sheet flows by Ollier and Brown (1965). Unless rootless vents feed new breakouts from the tube, thereby thickening the flow by stacking of smaller breakout lobes (Mattox et al., 1993), lava will be delivered through the sheet to the ocean with little change to the plateau. Thus, once a stable pathway across the plains is established to the coast, inflation essentially ceases unless the pathway structure is ruptured or blocked and begins the process of flow emplacement on the surface again.

As inflation of the sheet occurs, depressions form in places that experience little or no inflation, typically where previously high standing terrain inhibited the establishment of a continuous liquid core (Walker, 1991, 2009; Self et al., 1998). The resultant morphology comprises broad, smooth to hummocky plateaus with irregular shaped depressions of various depths (Chitwood, 1994) known as lava-rise pits (Walker, 1991, 2009; Self et al., 1998). Plateau margins are often defined by steeply tilted crust that is separated from the upper plateau by cracks, or inflation clefts, or a gently sloping margin with minor clefts or a series of stacked lobes and toes. This style of cracking, or cleft formation, is necessary to accommodate crust extension between the static margins and the inflating interior (Walker, 1991; Hon et al., 1994; Keszthelyi et al., 2004; Hoblitt et al., 2012).

Inflation can also be focused along the roof of a lava tube or narrow pathway within a sheet depending on the specific emplacement conditions (Hon et al., 1994; Cashman and Kauahikaua, 1997). Recent observations of flows emplaced during an episode in late 2010 show that tube-related inflation can occur when a relatively low local emplacement rate enables the flow to be laterally-confined by local, small-scale topography (Orr et al., 2015). In this case, lateral spreading is inhibited due to obstacles, and the confined flow field remains narrow and can form a tube. Much like inflated sheets, tubes on low slopes have little or no void space between the roof and liquid lava core. As such, the tube roof will experience inflation when the liquid core and thickening crust remain coupled while lava is delivered to the advancing flow front (Hamilton et al., 2013). Because the entire local flux of lava becomes focused into this narrow pathway, only the tube roof experiences inflation-related uplift, thereby producing a ridge along the axis of the tube. Unlike broad, flat-topped inflation plateaus that exhibit clefts along their margins, ridges display a large central cleft or group of axial clefts (Orr et al., 2015). Due to a similar inflation origin, clefted ridges can, in theory, attain heights or thicknesses as large as inflation plateaus.

Lava tubes on low slope plains also experience breakouts as observed on higher slope flank tubes. Plains tubes tend to experience periodic breakouts from the flanks of the clefted ridges during periods of increased lava flux through the system (Orr et al., 2015). Thus, small breakout lobes are emplaced adjacent to a ridge, rather than directly above the tube through the clefts. As the tube roof uplifts it is synchronously partly buried by its own outbreaks, resulting in a narrow clefted ridge trending along the crest of a broad, low profile rise comprised of small breakout lobes. Together a sinuous tumulus and broad rise compose a flow field that is called a sinuous, elongate tumulus (Hon et al., 1994; Cashman and Kauahikaua, 1997; Orr et al., 2015) or flow lobe tumulus (Rossi and Gudmundsson, 1996).

Observations of lava emplacement from the Pu‘u ‘Ō‘ō vent since 1981 show that lava flows encountering a change in slope from steep to shallow do not always produce fan deposits. Depending on the emplacement rate, the active flow front can spread laterally and subsequently produce a variety of inflation-related features, such as ridges and plateaus as opposed to fans. Orr et al. (2015) observed a tube-fed lava flow on the main flank of Kīlauea transition into an inflating ridge on the low slope coastal plain. Where not bound by existing topography, advance of lava across the low-slope plain involved a thin and broad flow front composed of small breakout toes. However, where the advancing lava was confined by older inflated lava flows or fault scarps, lateral advancement was inhibited and a narrow pathway or tube formed. Inflation of the tube roof followed over the next several months producing a pronounced ridge with a central cleft (clefted ridge) that was situated along the axis of a broad, low profile rise composed of breakouts from the base of the clefted ridge (Orr et al., 2015). This low slope lava tube morphology results from nearly continuous coupling of the liquid within the tube and the tube roof and walls, meaning that the tube continued to flow at full capacity most, if not all, of the time and experienced only minor breakouts at the base of the inflated roof. Sinuous elongate tumuli (i.e., a clefted ridge and broad rise) formation represents a fairly stable episode of lava emplacement with respect to the local lava flux through the transport system. Large fluctuations in flux or pulses of lava through the system can cause tube disruption such as shatter ring formation (Orr, 2010) or breakouts and rootless vent formation (Patrick and Orr, 2011) thereby leading to the establishment of new surface pathways (such as lava channels) and the abandonment of the elongate sinuous tumulus.

Perhaps the best example of an elongate sinuous tumulus involves the informally named Kahauale‘a flows (Patrick et al., 2015), which formed as the Pu‘u ‘Ō‘ō lavas began flowing to the northeast in 2013. These flows threatened to inundate the town of Pāhoa before the flow field experienced breakouts up slope that diverted the active flow fronts to new locations (Poland et al., 2016). As the flow entered the outskirts

of Pāhoa the narrowly confined flow field experienced inflation along the axis of the active pathway. Much as the elongate sinuous tumulus formed on the coastal plains south of Puʻu ʻŌʻō in 2010 (Orr et al., 2015) this flow field experienced narrow inflation coupled with localized breakouts along the flow field's lateral margins producing a clefted ridge over a broad rise composed of small breakout lobes (Fig. 11). However, in this case the flow field morphology is easier to observe because the flow advanced over grassy fields opposed to older basalt of the same color.

Inflation of lava sheets can also be inferred at older lava flows along the Hawaiian coastal plain, such as at the Mauna Loa 1859 lava flow (Fig. 12). The morphology of this flow has been studied on the higher slope flank of Mauna Loa where it developed a paired pāhoehoe and ʻaʻā channel based on changes in eruption and emplacement conditions (Rowland and Walker, 1990). The flow has been studied separately where the flow front advanced across the low slope coastal plain (Walker, 1991, 2009). Here, the flow widens considerably and all traces of the channel transport system are lost. The morphology evolves into a series of high-standing plateaus that rise 2–5 m above the surrounding hummocky lava surfaces. Within the plateaus are circular to irregular shaped depressions that are on the order of several meters deep, referred to as lava-rise pits by Walker (1991). The plateaus are most pronounced where the flow field, upon spreading across the coastal plain, flowed back towards the increased slope of Mauna Loa's flank. Here the lava became trapped between the thickening flow field towards the coast and the flank. The confinement by topography inhibited the lateral spreading of the flow front and enhanced sheet inflation.

Perhaps the best, if not the most commonly discussed, examples of paired ridge and plateau morphologies come from lava flows in North Queensland, Australia. The Undara and Toomba lava flows in the Cenozoic Eastern Australian Volcanic Zone reach 160 and 120 km in length respectively (Stephenson et al., 1998). Both flows display evidence for broad inflated plateaus. Undara displays a ridge ~43 km in length and 200-m-wide that rises up to 20 m above the surrounding lava (Stephenson et al., 1998). The Undara ridge, known as "The Wall", is surrounded by several kilometers of less inflated sheet flows (Stephenson and Whitehead, 1996). The Wall displays longitudinal furrows up to 10-m-wide along the upper surface and is inferred to have formed due to inflation comparable to the process observed by Orr et al. (2015). Stephenson et al. (1998) note that its sinuosity mimics the path of the nearby Junction Creek. Whitehead and Stephenson (1998) describe a ridge along the Toomba flow that rises nearly 7 m above the surrounding lava and varies from 35 m to 300 m in width, displaying abundant clefts and pits where the ridge is wider. They note that the Toomba ridges are present where the flow is located near the Burdekin River and is sometimes located between narrow stretches of two older lava flows, the Birdbush and Kangerong flows. They conclude that ridges are located where the flow appears to have flowed down older streambeds, leading to migration of the fluvial pathways to adjacent locations, and involved Hawaiian-like eruption rates with slow and steady emplacement. The presence of ridges where the advance of the Undara and Toomba flows followed preexisting narrow pathways between older, higher topography lava flows is consistent with the observations of Orr et al. (2015) that sinuous, elongate tumuli form via inflation where lateral spreading of a flow front is inhibited.

The terrestrial examples discussed here provide context from which to interpret the flow features observed in the plains east of Pavonis Mons. Keszthelyi et al. (2000) conclude that lava flows on planets with lower gravity are expected to experience more flow inflation. They state that inflation requires the formation of a coherent upper crust, continued lava supply, and conditions under which it is easier for the lava to move upward opposed to advancing laterally. The lower gravitational acceleration on Mars results in a decreased driving force for lateral advance and a decreased force resisting upward motion of the crust. Thus, in general it might be expected that lava inflation would be more common on Mars than on the Earth. Additionally, on Earth, lava flow ridges and plateaus are found in association with topographic features that physically inhibit lateral lava flow advance. Fig. 9 shows an example of a lava flow east of Pavonis Mons that encountered a low shield, or topographic obstacle. At this location the flow's morphology transitions into a broad, flat topped plateau with pits and steep sided margins as described by Walker (1991, 2009). Fig. 10 shows that plains lava flows often encountered not only vent structures but previously emplaced lava tubes and thick channelized lava flows. Hamilton et al. (2013) showed that inflating lobes can be affected by topography on the scale of the initial thickness of the toes at the lava flow front. Thus, the meters to 100 s meter thick lava channels and tubes, low shields and previously emplaced sinuous plains ridges and plateaus are more than sufficient to confine lava flows and initiate plateau and sinuous plains ridge formation.

Flows initially widen at the slope break, but width is highly variable along the flow lengths in relation to preexisting terrain. Crown and Baloga (1999) find that at the meter scale lava toes tend to be greater in length than width except on low slopes where toes tend to spread

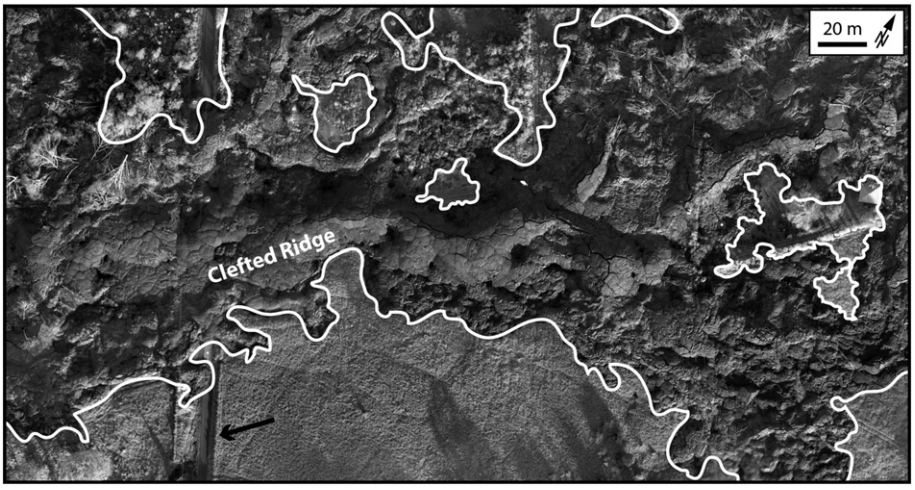

Fig. 11. Image mosaic showing the Kahauale'a flow at the western edge of the town of Pāhoa developed from images taken during UAV (Unmanned Aerial Vehicle) flights over the flow field. Here the flow field advanced as a tube-fed pāhoehoe flow via the breakout of small lobes at the flow front. As the front continued to advance a lava tube formed which subsequently experienced inflation of the roof producing a several meter high clefted ridge surrounded by small breakout lobes that define a broad rise. Together the clefted ridge and broad rise compose an elongate sinuous tumulus. The black arrow points to a street for scale. UAV imagery provided by Dr. Ryan L. Perroy, University of Hawai'i Hilo Spatial Data Analysis & Visualization (SDAV) laboratory.

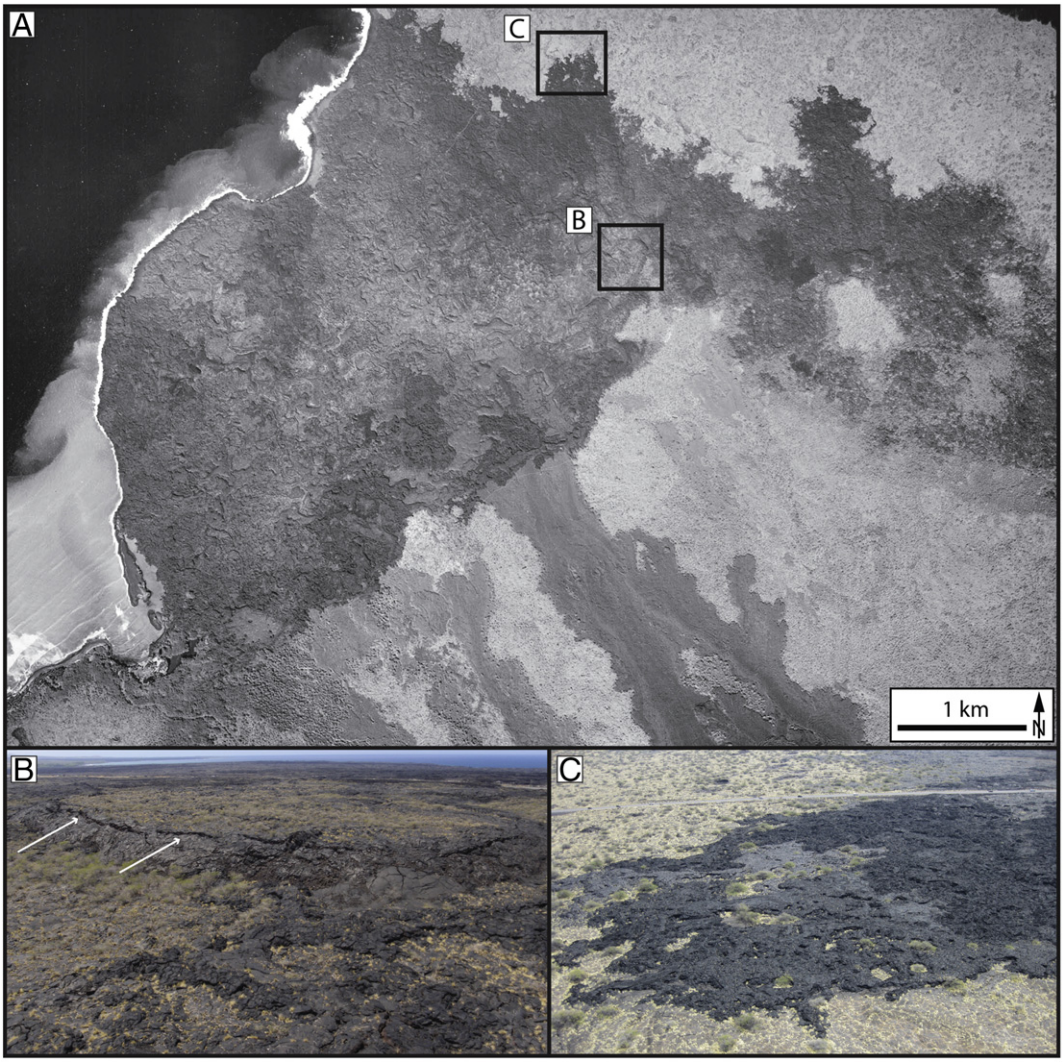

Fig. 12. The 1859 Mauna Loa flow formed both pāhoehoe and ʻaʻā channel segments where emplacement occurred across the several degree sloping flank of the volcano. The image in panel A shows the distal portion of the 1859 flow that covers the coastal plain, where the flow broadened significantly on the near zero degree slope. Panel B (inset marked in panel A) shows an oblique airborne view of a large inflated plateau margin within the 1859 sheet flow. Thin white arrows point upslope to the inflation clefts, above which the flat, smooth upper surface of the inflation plateau is visible. Panel C (inset marked in panel A) shows a section of the eastern margin of the 1859 sheet flow where flow advance involved small breakout lobes leaving behind small uncovered depressions, or kīpukas, which would have developed into lava rise inflation pits had this part of the flow experienced significant sheet inflation. The images shown in panels B and C were taken by the authors during a helicopter flight over the 1859 flow. The image shown in panel A is EKL-7CC-127 acquired on January 17, 1965 by the USDA Farm Service Agency, and this image is in the public domain.

laterally and can have higher widths than lengths. Peitersen and Crown (1999, 2000) find that at the flow field scale (>10 m) flows do not consistently widen on shallower slopes across the Hawaiian plains but conclude that topographic influences control the final width of a lava flow. Thus, field observations are consistent with Pavonis Mons lava flows transitioning from a higher slope rift apron onto a lower slope plain, initially broadening and advancing as a thin sheet before encountering local topography from older flows and vents that included relief that was high enough to confine flow field advance, and initiate inflation either narrowly as sinuous plains ridges or broadly as sheets.

The variable morphology of sinuous plains ridge is also consistent with lava flow emplacement. Ridges can form when long stretches of roof over a narrowly confined flow field experience inflation (see Fig. 7 of Orr et al. (2015)). Additionally, as the flow is advancing through and around obstacles a series of independent ponds or pools can develop. In this way the flow field can thicken by overflowing the ponds and producing short spillover flows. These small lobes stack to form a lower broad rise in much the same way that the breakouts along a terrestrial clefted ridge build an adjacent broad rise, which together define a sinuous elongate tumulus. Narrow flow fields that display a series of perched ponds are referred to as perched lava channels and have been observed to produce ridges that rise 10 s of meters above the pre-flow terrain (Patrick et al., 2011). The variations in ridge morphology in the Tharsis plains suggests that lava flows experienced different emplacement conditions throughout their path, sometimes transitioning from broad sheet flows to narrowly confined lobes. These flows appear to have developed pools and ponds along their pathway, some of which experienced inflation to produce sinuous plains ridges, or sinuous elongate tumuli and some of which likely remained opened for periods of time as channels developed into perched channels. The observation of small ridges within the floors of broader ridge tops (Fig. 8) suggests that locally some of these processes changed over time. It is possible that perched channels could have later developed internal pathways that subsequently acted as an elongate sinuous tumulus.

The interpretation of the plains plateaus and ridges as inflationary lava flow features is inconsistent in one way with observations of terrestrial inflated lava flows. No cracks or inflation clefts are observed in the study area, as required on Earth for a flow's brittle crust to accommodate endogenous growth via inflation (Walker, 1991; Hon et al., 1994; Keszthelyi et al., 2004; Hoblitt et al., 2012). Garry et al. (2012) discuss

a similar problem when suggesting that the Ina D feature on the Moon is associated with lava flow inflation. At that site a series of smooth-topped plateaus within a larger depression are suggested by Garry et al. (2012) to have formed via lava inflation, but no clefts are present. The Tharsis region of Mars is well known to be covered by a pervasive dust deposit (Ruff and Christensen, 2002) thick enough to obscure orbital spectral observations, and in high resolution image data dust mantles are often seen to mute or completely bury surface textural information beneath dunes. Observations of inflated lava flows in the arid southwest of the United States of America suggest that inflation clefts tend to accumulate aeolian deposits, nearly completely obscuring their presence within 10 s to 100 s of thousands of years (Fig. 13). In a region of Mars that is so heavily covered in dust, it is possible that inflation clefts along sheet flow margins would be filled to the point that they are not detectable remotely. Furthermore, some of the double crested ridges might represent inflation clefts along sinuous tumuli. Research related to aeolian deposition rates and the burial of inflation-related clefts is a topic for future research to support our understanding of the lava flow emplacement and subsequent modification history in the Tharsis region.

6. Conclusions

The main flanks and younger rift aprons of the Tharsis Montes display ample evidence for basaltic lava flow emplacement, as based on morphologic interpretations. Unlike the main flanks, the rift aprons also display sinuous and sometimes branching channel networks that lack levees and have been suggested to be the result of erosion, potentially resulting from fluvial processes. The >1° sloping rift aprons transition to <1° sloping Tharsis plains. This study focused on the morphologic relationship between the southwest rift apron of Pavonis Mons and the plains units to the east in order to understand the genetic relationship between the two terrains and to provide clues to the developmental history of the rift apron with respect to volcanism and possible fluvial processes.

Southeast trending flow units from the rift apron that extend across this steep-to-shallow slope break do not display fan deposits but instead widen and become smooth over a distance of several kilometers before reestablishing channel or tube morphologies that trend to the northeast. Whereas sinuous and branching, non-leveed channel networks are interspersed among channels and tubes on the rift apron, sinuous plains ridges and plateaus, which are sometimes linked, are interspersed among the channels and tubes of the plains units. Basaltic ridges and plateaus on the Earth are indicative of lava inflation processes, either focused along sinuous branches of lava tubes or broadly across sheet flows. If the local volumetric flow rate is low enough that flows can be confined by local topography (e.g., already emplaced flow margins or fault scarps), then the resultant lava flows are narrow and can quickly form lava tubes along which inflation is focused at the tube roof. The resultant morphology is a sinuous, elongate ridge or tumulus. Flows advancing in this manner, controlled by inflation, produce plateaus that are interspersed with sinuous ridges.

Lava flows >100 km in length are observed across Tharsis (Zimbelman, 1998; Baloga et al., 2003; Garry et al., 2006; Crown and Ramsey, 2017). Keszthelyi and Self (1998) conclude that long lava flows (>100 km) emplaced across low slopes (<5°) require either

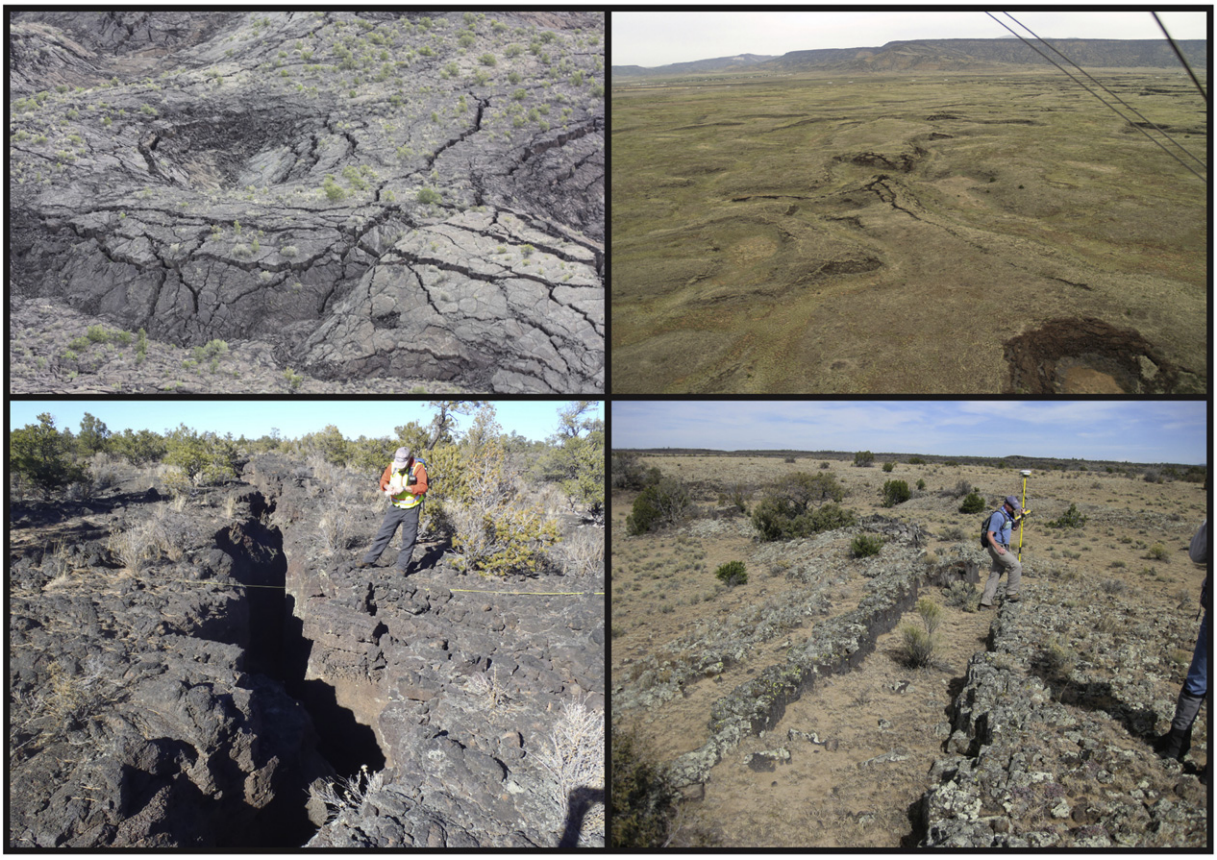

Fig. 13. The development of inflated lava flows involves the formation of large cracks or clefts to accommodate spreading of the brittle crust. All images in this figure show inflated plateaus within lava flows in the Zuni-Bandera volcanic field, NM. The images shown in panels A and B were acquired by the authors during light sport aircraft trike flights at an altitude of ~120–150 m, showing the 2000–4000 year old McCartys lava flow field (A) and the ~115,000 year old El Calderon flow field (B). The images shown in panels C and D were acquired by the authors on the ground and show inflation clefts in the McCartys flow field (C) and the 10,000–19,000 year old Hoya de Cibola flow field (flow ages are from Maxwell, 1986; Laughlin et al., 1993, 1994, Laughlin and WoldeGabriel, 1997; Dunbar and Phillips, 2004). Panels A and C from the McCartys flow show relatively unmodified clefts, whereas panels B and D show that inflation clefts can be nearly completely obscured by aeolian processes within 10,000 to 100,000 years in the Zuni-Bandera volcanic field.

(1) emplacement conditions consistent with rapid emplacement rates (local volumetric flow rate), or (2) insulated emplacement where heat loss is minimized. The observations presented here of plateau and ridge formation are consistent with the second scenario of Keszthelyi and Self (1998) involving long lava flow development across low slopes with emplacement styles that involve lava insulation. Several terrestrial examples have been discussed here with comparable plateau and ridge morphologies. Another terrestrial example is the >75 km long Carrizozo lava flow field in New Mexico, which also displays a narrow section with a sinuous ridge and a wider distal margin with broad plateaus (Keszthelyi and Pieri, 1993; Zimbelman and Johnston, 2001, 2003). Keszthelyi and Pieri (1993) infer that the Carrizozo lava flow field was emplaced over a period of at least three decades with eruption rates comparable to those in Hawai'i (5 $m^3 s^{-1}$), in agreement with the assertion that long lava flows with ridges and plateaus are evidence of relatively slow and insulated emplacement opposed to high eruption or local volumetric flow rates.

We interpret the sinuous plains ridges east of Pavonis Mons to share an analogous origin to terrestrial sinuous elongate tumuli (or low slope clefted ridges). The variable morphologies displayed by the Martian features suggest a formation history strongly linked to local emplacement (volumetric flow rate) and pre-flow topography that produced interspersed inflation plateaus, sinuous elongate tumuli, perched channels and lava channels and tubes that appear morphologically similar to those higher up on the flanks of Pavonis Mons. The presence of these features down-flow of the rift apron units leads us to conclude that many of the Tharsis plains ridges and plateaus are the product of rift apron lava flows that were emplaced across a steep-to-shallow slope break, thereby resulting in changes in morphology within the same flow field. These lava flows were likely emplaced in a slow and steady manner as seen on Earth, potentially experiencing minor changes in local volumetric flow rate conditions leading to minor, short breakouts from the established pathways. As these flows navigated through the topographic obstacles in the nearly flat plains they experienced lava flow inflation in several different manners depending on local conditions resulting in both ridges and plateaus. Sediment-laden fluvial flows or mudflows that encounter a steep-to-shallow slope break are expected to deposit their sedimentary load. Thus, a lack of fan deposits in locations where rift apron flows transition across the slope break is not consistent with a fluvial origin of the rift apron units. However, a lack of fan deposits at this slope break is consistent with rift apron lavas emplaced at a low local volumetric flow that, upon advancing onto a lower slope surface, spread laterally across the Tharsis plains and inflated to produce plateaus and ridges.

Sinuous ridges found elsewhere across the surface of Mars are interpreted as inverted fluvial channels (Malin and Edgett, 2003; Mangold et al., 2004; Moore and Howard, 2005; Pain et al., 2007; Burr et al., 2009, 2010; Williams et al., 2009; Anderson and Bell, 2010; Zimbelman and Griffin, 2010; Le Deit et al., 2010; Weitz et al., 2010; Newsom et al., 2010; Thomson et al., 2011; Ansan et al., 2011; Lefort et al., 2012), eskers (Baker, 2001; Head and Pratt, 2001; Bleacher et al., 2003; Ghatan and Head, 2004; Banks et al., 2009; Williams et al., 2013), or eroded remnants of subsurface dikes (Head et al., 2006). The development of inverted fluvial channels and eskers involves flowing water, and all three of these proposed processes require significant erosion and regional deflation. The study area is not a region thought to have experienced significant sedimentary deposition or subsequent erosion (Tanaka et al., 2014). It is highly unlikely that 10 s of meters of basaltic lava flow material has been removed across the Tharsis plains in the last several hundred mission years in a manner that would produce inverted fluvial terrains. However, Bleacher et al. (2013) and Orr et al. (2015) suggested that some sinuous ridges in the eastern Tharsis plains were the result of lava flow emplacement. Subsequently, Zhao et al. (2015) proposed a comparable volcanic origin for ridges in the Solis Planum region and Crown and Ramsey (2017) observe similar features that they also attribute to lava flow emplacement to the southwest of Arsia Mons. The interpretation of some sinuous ridges on Mars as sinuous elongate tumuli that form over narrow lava pathways provides an alternative hypothesis for Mars sinuous ridge formation. We do not propose that this hypothesis explains all other examples of Martian sinuous ridges. As stated by Williams et al. (2013), "The morphological characteristics and geologic context for each sinuous ridge must be assessed to accurately interpret the formation history of the landform and infer associated climatic conditions."

Within the geologic context of the eastern Tharsis plains adjacent to Pavonis Mons, sinuous plains ridges that are linked with plateaus are consistent with a formation via slow and steady lava flow emplacement across low slope terrains through ample topographic obstacles that acted to inhibit lateral flow field advance. Both plateaus and ridges are indicative of flow inflation either across broad sheets or topographically confined, narrow pathways. Because these units are linked with units on the rift apron of Pavonis Mons, we also conclude that those units share a volcanic origin, including sinuous and branching, non-leveed channel networks. As observed on Earth, a volcanic eruption that emplaces lava through a range of regional slopes and assortment of local topographic obstacles can produce a variety of lava flow pathway structures and morphologies, which is consistent with the transition in lava flow structures observed throughout the study area.

Acknowledgements

We thank journal reviewers David Crown and Ernst Hauber for their constructive comments that improved the content and presentation of this research. We also thank Laszlo Keszthelyi and Rebecca Williams for additional recommendations that helped clarify the conclusions presented here. Funding for this project was provided by multiple sources, including NASA Mars Data Analysis Program (MDAP) project 12-MDAP12-0013 funding to J. Bleacher and NASA Planetary Geology and Geophysics grant # NNX14AL54G to C. Hamilton. W.B. Garry and D. Williams were in part supported by MDAP 09-MDAP09-0020. T. Orr's funding is provided by the U.S. Geological Survey's Volcano Hazard Program. Field work conducted in Hawai'i on Kīlauea volcano and in New Mexico at the Zuni-Bandera Volcanic Field was supported by NASA's Moon and Mars Analog Mission Activities proposal 08-MMAMA08-0016. Field work at both sites is supported by National Park Service research permits HAVO-2012-SCI-0025 and HAVO-2016-SCI-0005 as well as ELMA-2015-SCI-0001, respectively.

References

Anderson, R.B., Bell, J.F., 2010. Geologic mapping and characterization of Gale Crater and implications for its potential as a Mars Science Laboratory landing site. Mars 5: 76–128. http://dx.doi.org/10.1555/mars.2010.0004.

Ansan, V., Loizeau, D., Mangold, N., Le Mouelic, S., Carter, J., Poulet, F., Dromat, G., Lucas, A., Bibring, J.-P., Gendrin, A., Gondet, B., Langevin, Y., Masson, Ph., Murchie, S., Mustard, J.F., Neukum, G., 2011. Stratigraphy, mineralogy, and origin of layered deposits inside Terby crater, Mars. Icarus 211:273–304. http://dx.doi.org/10.1016/j.icarus.2010.09.011.

Bailey, J.E., Harris, A.J.L., Dehn, J., Calvari, S., Rowland, S.K., 2006. The changing morphology of an open lava channel on Mt. Etna. Bull. Volcanol. 68:497–515. http://dx.doi.org/10.1007/s00445-005-0025-6.

Baker, V.R., 2001. Water and the Martian landscape. Nature 412 (6843), 228–236.

Baker, V.R., Hamilton, C.W., Burr, D.M., Gulick, V.C., Komatsu, G., Luo, W., Rice Jr., J.W., Rodriguez, J.A.P., 2015. Fluvial geomorphology on Earth-like planetary surfaces: a review. Geomorphology 245:149–182. http://dx.doi.org/10.1016/j.geomorph.2015.05.002.

Baloga, S.M., Glaze, L.S., 2008. Self-replication model for long channelized lava flows on the Mars plains. J. Geophys. Res. 113, E05003. http://dx.doi.org/10.1029/2007JE002954.

Baloga, S.M., Mouginis-Mark, P.J., Glaze, L.S., 2003. Rheology of a long lava flow at Pavonis Mons, Mars. J. Geophys. Res. 2018, E750006. http://dx.doi.org/10.1029/2002JE001981.

Banks, M.E., Lang, N.P., Kargel, J.S., McEwen, A.S., Baker, V.R., Grant, J.A., Pelletier, J.D., Strom, R.G., 2009. An analysis of sinuous ridges in the southern Argyre Planitia, Mars using HiRISE and CTX images and MOLA data. J. Geophys. Res. 114 (E9), E09003. http://dx.doi.org/10.1029/2008JE003244.

Baptista, A.R., Mangold, N., Ansan, V., Baratoux, D., Lognonné, P., Alves, E.I., Williams, D.A., Bleacher, J.E., Masson, P., Neukum, G., 2008. A swarm of small shield volcanoes on

Syria Planum, Mars. J. Geophys. Res. 113, E09010. http://dx.doi.org/10.1029/2007JE002945.
Baratoux, D., Pinet, P., Toplis, M.J., Mangold, N., Greeley, R., Baptista, A.R., 2009. Shape, rheology and emplacement times of small Martian shield volcanoes. J. Volcanol. Geotherm. Res. 185:47–68. http://dx.doi.org/10.1016/j.jvolgeores.2009.05.003.
Bleacher, J.E., Greeley, R., 2008. Relating volcano morphometry to the developmental progression of Hawaiian shield volcanoes through slope and hypsometric analyses of SRTM data. J. Geophys. Res. 113, B09208. http://dx.doi.org/10.1029/2006JB004661.
Bleacher, J.E., Sakimoto, S.E.H., Garvin, J.B., Wong, M., 2003. Deflation/erosion rates for the Parva Member, Dorsa Argentea Formation and implications for the south polar region of Mars. J. Geophys. Res. 108 (E7):5075. http://dx.doi.org/10.1029/2001JE001535.
Bleacher, J.E., Greeley, R., Williams, D.A., Cave, S.R., Neukum, G., 2007a. Trends in effusive style at the Tharsis Montes, Mars, and implications for the development of the Tharsis province. J. Geophys. Res. 112, E09005. http://dx.doi.org/10.1029/2006JE002873.
Bleacher, J.E., Greeley, R., Williams, D.A., Werner, S.C., Hauber, E., Neukum, G., 2007b. Olympus Mons, Mars: inferred changes in late Amazonian aged effusive activity from lava flow mapping of Mars Express High Resolution Stereo Camera data. J. Geophys. Res. 112, E04003. http://dx.doi.org/10.1029/2006JE002826.
Bleacher, J.E., Glaze, L.S., Greeley, R., Hauber, E., Baloga, S.M., Sakimoto, S.E.H., Williams, D.A., Glotch, T.D., 2009. Spatial and alignment analyses for a field of small volcanic vents south of Pavonis Mons and implications for the Tharsis province, Mars. J. Volcanol. Geotherm. Res. 185:96–102. http://dx.doi.org/10.1016/j.jvolgeores.2009.04.008.
Bleacher, J.E., Orr, T.R., Garry, W.B., Hamilton, C.W., Zimbelman, J.R., de Wet, A., 2013. Sinuous ridges and plateaus as evidence for lava flow inflation in the Tharsis plains of Mars: insights from analogous features on the coastal plain of Kilauea Volcano, HI. 44th Lunar and Planetary Science Conference, Abstract 2090. Lunar and Planetary Institute, Houston.
Brož, P., Hauber, E., 2012. A unique volcanic field in Tharsis, Mars: pyroclastic cones as evidence for explosive eruptions. Icarus 218:88–99. http://dx.doi.org/10.1016/j.icarus.2011.11.030.
Brož, P., Čadek, O., Hauber, E., Rossi, A.P., 2014. Shape of scoria cones on Mars: insights from numerical modeling of ballistic pathways. Earth Planet. Sci. Lett. 406:14–23. http://dx.doi.org/10.1016/j.epsl.2014.09.002.
Burr, D.M., Bruno, B.C., Lanagan, P.D., Glaze, L.S., Jaeger, W.L., Soare, R.J., Wan Bun Tseung, J.-M., Skinner Jr., J.A., Baloga, S.M., 2009. Mesoscale raised rim depressions (MRRDs) on Earth: a review of the characteristics, processes, and spatial distributions of analogs for Mars. Planet. Space Sci. 57, 579–596.
Burr, D.M., Williams, R.M.E., Wendell, K.D., Chojnacki, M., Emery, J.P., 2010. Inverted fluvial features in the Aeolis/Zephyria Plana region, Mars: formation mechanism and initial paleodischarge estimates. J. Geophys. Res. 115 (E7), E07011. http://dx.doi.org/10.1029/2009JE003496.
Calvari, S., Pinkerton, H., 1998. Formation of lava tubes and extensive flow field during the 1991–1993 eruption of Mount Etna. J. Geophys. Res. B103, 27291–27301.
Calvari, S., Pinkerton, H., 1999. Lava tube morphology on Etna and evidence for lava flow emplacement mechanisms. J. Volcanol. Geotherm. Res. 90, 263–280.
Carr, M.H., Greeley, R., 1980. Volcanic Features of Hawaii: A Basis for Comparison With Mars. NASA SP-403. US Government Printing Office, Washington, D.C. (211 pp.).
Carr, M.H., Greeley, R., Blasius, K.R., Guest, J.E., Murray, J.B., 1977. Some Martian volcanic features as viewed from the Viking Orbiter. J. Geophys. Res. 82 (28), 3985–4015.
Cashman, K.J., Kauahikaua, J.P., 1997. Reevaluation of vesicle distributions in basaltic lava flows. Geology 25 (5), 419–422.
Cashman, K.V., Thornber, C., Kauahikaua, J.P., 1999. Cooling and crystallization of lava in open channels, and the transition of pahoehoe to aa. Bull. Volcanol. 61, 306–323.
Chitwood, L.A., 1994. Inflated basaltic lava—examples of processes and landforms from central and southeast Oregon. Or. Geol. 56, 11–21.
Christensen, P.R., Jakosky, B.M., Kieffer, H.H., Malin, M.C., McSween, H.Y., Nealson, K., Mehall, G.L., Silverman, S.H., Ferry, S., Caplinger, M., Ravine, M., 2004. The Thermal Emission Imaging System (THEMIS) for the Mars 2001 Odyssey Mission. Space Sci. Rev. 110, 85–130.
Crown, D.A., Baloga, S.M., 1999. Pāhoehoe toe dimensions, morphology, and branching relationships at Mauna Ulu, Kīlauea Volcano, Hawaii. Bull. Volcanol. 61:288–305. http://dx.doi.org/10.1007/s004450050298.
Crown, D.A., Ramsey, M.S., 2017. Morphologic and thermophysical characteristics of lava flows Southwest of Arsia Mons, Mars. J. Volcanol. Geotherm. Res. 342, 13–28.
Crumpler, L.S., Aubele, J.C., Zimbelman, J.R., 2007. Volcanic features of New Mexico analogous to volcanic features on Mars. In: Chapman, M.G. (Ed.), The Geology of Mars: Evidence from Earth-based Analog. Cambridge University Press, Cambridge, UK (ISBN-13 978-0-521-83292-2 (HB)).
Dunbar, N.W., Phillips, F.M., 2004. Cosmogenic ^{36}Cl ages of lava flows in the Zuni–Bandera volcanic field, north–central New Mexico, U.S.A. Bull. New Mex. Bur. Min. Mineral Resour. 160, 309–317.
Garry, W.B., Zimbelman, J.R., Gregg, T.K.P., 2007. Morphology and emplacement of a long channeled lava flow near Ascraeus Mons, Mars. J. Geophys. Res. 112, E08007. http://dx.doi.org/10.1029/2006JE002803.
Garry, W.B., Robinson, M.S., Zimbleman, J.R., Bleacher, J.E., Hawke, B.R., Crumpler, L.S., Braden, S.E., Sato, H., 2012. The origin of Ina: evidence for inflated lava flows on the Moon. J. Geophys. Res. 117. http://dx.doi.org/10.1029/2011JE003981.
Glaze, L.S., Baloga, S.M., Garry, W.B., Fagents, S.A., Parcheta, C., 2009. A hybrid model for leveed lava flows: implications for eruption styles on Mars. J. Geophys. Res. 114, E07001. http://dx.doi.org/10.1029/2008JE003278.
Glaze, L.S., Baloga, S.M., 2006. Rheologic inferences from the levees of lava flows on Mars. J. Geophys. Res. 111, E09006. http://dx.doi.org/10.1029/2005JE002585.
Ghatan, G.J., Head III, J.W., 2004. Regional drainage of meltwater beneath a Hesperian aged south circumpolar ice sheet on Mars. J. Geophys. Res. 109 (E7), E07006. http://dx.doi.org/10.1029/2003JE002196.
Giacomini, L., Carli, C., Sgavetti, M., Massironi, M., 2012. Spectral analysis and geological mapping of the Daedalia Planum lava field (Mars) using OMEGA data. Icarus 220, 679–693.
Greeley, R., 1971. Observations of actively forming lava tubes and associated structures, Hawaii. Mod. Geol. 2, 207–223.
Greeley, R., 1972. Additional observations of actively forming lava tubes and associated structures, Hawaii. Mod. Geol. 3, 157–160.
Greeley, R., 1987. The role of lava tubes in Hawaiian volcanoes. In: Decker, R.W., Wright, T.L., Stauffer, P.H. (Eds.), Volcanism in Hawaii. U.S. Geol. Surv. Prof. Pap. vol. 1350(2), pp. 1589–1602.
Greeley, R., Spudis, P.D., 1981. Volcanism on Mars. Rev. Geophys. Space Phys. 19:13–41. http://dx.doi.org/10.1029/RG019i001p00013.
Hamilton, C., Glaze, L., James, M., Baloga, S., 2013. Topographic and stochastic influences on pāhoehoe lava lobe emplacement. Bull. Volcanol. 75 (11):1–16. http://dx.doi.org/10.1007/s00445-013-0756-8.
Harris, A.J.L., Rowland, S.K., 2009. Effusion rate controls on lava flow length and the role of heat loss: a review. In: Thordarson, T., Self, S., Larsen, G., Rowland, S.K., Hoskuldsson, A. (Eds.), Studies in Volcanology—The Legacy of George Walker (Special Publications of IAVCEI No. 2). The Geol. Soc., pp. 33–51.
Harris, A.J.L., Dehn, J., Calvari, S., 2007. Lava effusion rate definition and measurement: a review. Bull. Volcanol. 70:1–22. http://dx.doi.org/10.1007/s00445-007-0120-y.
Hauber, E., Bleacher, J., Gwinner, K., Williams, D., Greeley, R., 2009. The topography and morphology of low shields and associated landforms of plains volcanism in the Tharsis region of Mars. J. Volcanol. Geotherm. Res. 185:69–95. http://dx.doi.org/10.1016/j.jvolgeores.2009.04.015.
Hauber, E., Brož, P., Jagert, F., Jodłowski, P., Platz, T., 2011. Very recent and wide-spread basaltic volcanism on Mars. Geophys. Res. Lett. 38, L10201. http://dx.doi.org/10.1029/2011GL047310.
Head III, J.W., Pratt, S., 2001. Extensive Hesperian-aged south polar ice sheet on Mars: evidence for massive melting and retreat, and lateral flow and ponding of meltwater. J. Geophys. Res. 106 (E6):12275–12299. http://dx.doi.org/10.1029/2000JE001359.
Head, J.W., Wilson, L., Dickson, J., Neukum, G., 2006. The Huygens-Hellas giant dike system on Mars: implications for Late Noachian–Early Hesperian volcanic resurfacing and climatic evolution. Geology 34 (4):285–288. http://dx.doi.org/10.1130/G22163.1.
Healy, B.F., Zimbelman, J.R., 2016. Mapping and studying inflated lava flows in Mars' Tharsis region. 47th Lunar and Planetary Science Conference, Abstract 1613. Lunar and Planetary Institute, Houston.
Heliker, C., Mattox, T.N., 2003. The first two decades of the Pu'u 'Ō'ō–Kupaianaha eruption; chronology and selected bibliography. In: Heliker, C., Swanson, D.A., Takahashi, T.J. (Eds.), The Pu'u 'Ō'ō—Kupaianaha Eruption of Kīlauea Volcano, Hawai'i: The first 20 years. U.S. Geol. Surv. Prof. Pap. 1676, pp. 1–27.
Helz, R.T., Hon, K.A., Heliker, C.C., 1993. In: Duggan, M.B., Knutson, Jan (Eds.), Thermal efficiency of lava tubes at Kilauea Volcano, Hawaii [abs.]. Ancient Volcanism & Modern Analogues: IAVCEI General Assembly, Canberra, Australia, 1993, Abstracts 1, no. 1, p. 47.
Helz, R.T., Thornber, C.R., 1987. Geothermometry of Kilauea Iki lava lake, Hawaii. Bull. Volcanol. 49 (5), 651–668.
Hiesinger, H., Head III, J.W., Neukum, G., 2007. Young lava flows on the eastern flank of Ascraeus Mons: rheological properties derived from High Resolution Stereo Camera (HRSC) images and Mars Orbiter Laser Altimeter (MOLA) data. J. Geophys. Res. 112, E05011. http://dx.doi.org/10.1029/2006JE002717.
Hoblitt, R.P., Orr, T.R., Heliker, C., Denlinger, R.P., Hon, K., Cervelli, P.F., 2012. Inflation rates, rifts, and bands in a pāhoehoe sheet flow. Geosphere 8 (1):179–195. http://dx.doi.org/10.1130/GES00656.1.
Hodges, C.A., Moore, H.J., 1994. Atlas of volcanic landforms on Mars. USGS Prof. Paper 1534. U. S. Govt. Printing Office, Washington, D.C.
Holcomb, R.T., 1987. Eruptive history and long-term behavior of Kilauea Volcano. In: Decker, R.W., et al. (Eds.), Volcanism in Hawaii. U.S. Geol. Surv. Prof. Pap. vol. 1350, pp. 261–350.
Hon, K., Kauahikaua, J., Denlinger, R., Mackay, K., 1994. Emplacement and inflation of pahoehoe sheet flows: observations and measurements of active lava flows on Kilauea Volcano, Hawaii. Geol. Soc. Am. Bull. 106 (3), 351–370.
Hulme, G., 1974. Interpretation of lava flow morphology. Geophys. J. R. Astron. Soc. 39, 361–383.
Kauahikaua, J., Cashman, K.V., Mattox, T.N., Heliker, C.C., Hon, K.A., Mangan, M.T., Thornber, C.R., 1998. Observations on basaltic lava streams in tubes from Kilauea Volcano, island of Hawai'i. J. Geophys. Res. 103 (B11):27303–27323. http://dx.doi.org/10.1029/97JB03576.
Kauahikaua, J., Sherrod, D.R., Cashman, K.V., Heliker, C., Hon, K., Mattox, T.N., Johnson, J.A., 2003. Hawaiian lava-flow dynamics during the Puu Oo-Kupaianaha eruption: a tale of two decades. In: Heliker, C., et al. (Eds.), The Puu Oo - Kupaianaha Eruption of Kilauea Volcano, Hawaii, the First 20 Years. U.S. Geol. Surv. Prof. Pap. 1676, pp. 63–87.
Keszthelyi, L., 1995. A preliminary thermal budget for lava tubes on the Earth and planets. J. Geophys. Res. 100 (B10):20,411–20,420. http://dx.doi.org/10.1029/95JB01965.
Keszthelyi, L.P., 2013. A facies model for primary mafic volcanic deposits. 44th Lunar and Planetary Science Conference, Abstract 2567. Lunar and Planetary Institute, Houston.
Keszthelyi, L., Pieri, D.C., 1993. Emplacement of the 75-km-long Carrizozo lava flow field, south-central New Mexico. J. Volcanol. Geotherm. Res. 59:59–75. http://dx.doi.org/10.1016/0377-0273(93)90078-6.
Keszthelyi, L., Self, S., 1998. Some physical requirements for the emplacement of long basaltic lava flows. J. Geophys. Res. 103 (B11):27447–27464. http://dx.doi.org/10.1029/98JB00606.

Keszthelyi, L., McEwen, A.S., Thordarson, T., 2000. Terrestrial analogs and thermal models for Martian flood lavas. J. Geophys. Res. 105 (E6):15,027–15,049. http://dx.doi.org/10.1029/1999JE001191.
Keszthelyi, L., Thordarson, T., McEwen, A., Haack, H., Guibaud, N., Self, S., Rossi, M.J., 2004. Icelandic analogs to Martian flood lavas. Geochem. Geophys. Geosyst. 5, Q11014. http://dx.doi.org/10.1029/2004GC000758.
Kilburn, C.R.J., 2000. Lava flows and flow fields. In: Sigurdsson, H., Houghton, B., Rymer, H., Stix, J. (Eds.), Encyclopedia of Volcanoes. Academic Press, London, pp. 291–305.
Koeppen, W.C., Patrick, M., Orr, T., Sutton, A.J., Dow, D., Wright, R., 2013. Constraints on the partitioning of Kīlauea's lavas between surface and tube flows, estimated from infrared satellite data, sulfur dioxide emission rates, and field observations. Bull. Volcanol. 75:716. http://dx.doi.org/10.1007/s00445-013-0716-3.
Lang, N.P., Tornabene, L.L., McSween, H.Y., Christensen, P.R., 2009. Tharsis-sourced relatively dust-free lavas and their possible relationship to Martian meteorites. J. Volcanol. Geotherm. Res. 185:103–115. http://dx.doi.org/10.1016/j.jvolgeores.2008.12.014.
Laughlin, A.W., WoldeGabriel, G., 1997. Dating the Zuni-Bandera volcanic field, Natural history of El Malpais National Monument. New Mexico Bureau of Mines & Mineral Resources Bulletin vol. 156. New Mexico Bureau of Geology and Mineral Resources, Socorro, NM, United States, pp. 25–30.
Laughlin, A.W., Perry, F.V., WoldeGabriel, G., 1994. Geochronology and geochemistry of basalts of the Zuni-Bandera volcanic field; a review and update. Mexico Geology]–>N. M. Geol. 16, 60.
Laughlin, A.W., Perry, F.V., Damon, P.E., Shafiqullah, M., WoldeGabriel, G., McIntosh, W., Harrington, C.D., Wells, S.G., Drake, P.G., 1993. Geochronology of Mount Taylor, Cebollita Mesa, and Zuni–Bandera volcanic fields, Cibola County, New Mexico. Mexico Geology]–>N. M. Geol. 15 (4), 81–92.
Le Deit, L.L., Bourgeois, O., Mège, D., Hauber, E., Le Mouélic, S., Massé, M., Jaumann, R., Bibring, J.-P., 2010. Morphology, stratigraphy, and mineralogical composition of a layered formation covering the plateaus around Valles Marineris, Mars: implications for its geological history. Icarus 208:684–703. http://dx.doi.org/10.1016/j.icarus.2010.03.012.
Lefort, A., Burr, D.M., Beyer, R.A., Howard, A.D., 2012. Inverted fluvial features in the Aeolis-Zephyria Plana, western Medusae Fossae Formation, Mars: evidence for post-formation modification. J. Geophys. Res. 117 (E3), E03007. http://dx.doi.org/10.1029/2011JE004008.
Macdonald, G.A., 1956. Pahoehoe, aa, and block lava. Am. J. Sci. 251, 169–191.
Malin, M.C., 1980. Lengths of Hawaiian lava flows. Geology 8, 306.
Malin, M.C., Edgett, K.S., 2003. Evidence for persistent flow and aqueous sedimentation on early Mars. Science 302:1931–1934. http://dx.doi.org/10.1126/science.1090544.
Malin, M.C., Bell, J.F., Cantor, B.A., Caplinger, M.A., Calvin, W.M., Clancy, R.T., Edgett, K.S., Edwards, L., Haberle, R.M., James, P.B., Lee, S.W., Ravine, M.A., Thomas, P.C., Wolff, M.J., 2007. Context Camera Investigation on board the Mars Reconnaissance Orbiter. J. Geophys. Res. 112, E05S04. http://dx.doi.org/10.1029/2006JE002808.
Malin, M.C., Danielson, G.E., Ingersoll, A.P., Masursky, H., Veverka, J., Ravine, M.A., Soulanille, T.A., 1992. The Mars observer camera. J. Geophys. Res. 97 (E5), 7699–7718.
Mangold, N., Quantin, C., Ansan, V., Delacourt, C., Allemand, P., 2004. Evidence for precipitation on Mars from dendritic valleys in the Valles Marineris area. Science 305:78–81. http://dx.doi.org/10.1126/science.1097549.
Mark, R.K., Moore, J.G., 1987. Slopes of the Hawaiian Ridge. In: Decker, R.W., et al. (Eds.), Volcanism in Hawaii. U.S. Geol. Surv. Prof. Pap. 1350, pp. 101–108.
Mattox, T.N., Heliker, C., Kauahikaua, J., Hon, K., 1993. Development of the 1990 Kalapana flow field, Kilauea Volcano, Hawaii. Bull. Volcanol. 55 (6), 407–413.
Maxwell, C., 1986. Geological Map of El Malpais lava field and Surrounding Areas, Cibola County, New Mexico. vol. I-1595. United States Geological Survey Map.
McEwen, A.S., Eliason, E.M., Bergstrom, J.W., Bridges, N.T., Hansen, C.J., Delamere, W.A., Grant, J.W., Gulick, V.C., Herkenhoff, K.E., Keszthelyi, L., Kirk, R.L., Mellon, M.T., Squyres, S.W., Thomas, N., Weitz, C.M., 2007. MRO's high resolution imaging science experiment (HiRISE). J. Geophys. Res. 112, E05S02. http://dx.doi.org/10.1029/2005JE002605.
Moore, J.M., Howard, A.D., 2005. Large alluvial fans on Mars. J. Geophys. Res. 111, E04005. http://dx.doi.org/10.1029/2004JE002352.
Moore, J.G., Mark, R.K., 1992. Morphology of the island of Hawaii. GSA Today 2, 257–262.
Morris, E.C., Tanaka, K.L., 1994. Geologic maps of the Olympus Mons region of Mars, scale 1:2,000,000 and 1:1,000,000, USGS Misc. Inv. Series Map I-2327.
Mouginis-Mark, P.J., Christensen, P.R., 2005. New observations of volcanic features on Mars from the THEMIS instrument. J. Geophys. Res. 110, E08007. http://dx.doi.org/10.1029/2005JE002421.
Mouginis-Mark, P.J., Rowland, S.K., 2008. Lava flows at Arsia Mons, Mars: insights from a graben imaged by HiRISE. Icarus 198. http://dx.doi.org/10.1016/j.icarus.2008.06.015.
Mouginis-Mark, P.J., Wilson, L., Zuber, M.T., 1992. The physical volcanology of Mars. In: Kieffer, H.H., et al. (Eds.), Mars. The University of Arizona Press, Tucson, pp. 424–452.
Murray, J.B., van Wyk de Vries, B., Marquez, A., Williams, D.A., Byrne, P., Muller, J., Kim, J., 2010. Late-stage water eruptions from Ascraeus Mons volcano, Mars: implications for its structure and history. Earth Planet. Sci. Lett. 294:479–491. http://dx.doi.org/10.1016/j.epsl.2009.06.020.
Neukum, G., Jaumann, R., the HRSC Co-Investigator and Experiment Team, 2004. HRSC: The High Resolution Stereo Camera of Mars Express. Eur. Space Agency Spec. Publ., ESA-SP 1240 pp. 17–36.
Newsom, H.E., Lanza, N.L., Ollila, A.M., Wiseman, S.M., Rousch, T.L., Marzo, G.A., Tornabene, L.L., Okubo, C.H., Osterloo, M.M., Hamilton, V.E., Crumpler, L.S., 2010. Inverted channel deposits on the floor of Miyamoto crater, Mars. Icarus 205 (1):64–72. http://dx.doi.org/10.1016/j.icarus.2009.03.030.
Ollier, C.D., Brown, M.C., 1965. Lava caves of Victoria (Australia). Bull. Volcanol. 28, 215–229.
Orr, T.R., 2010. Lava tube shatter rings and their correlation with lava flux increases at Kīlauea Volcano, Hawai'i. Bull. Volcanol. http://dx.doi.org/10.1007/s00445-010-0414-3.
Orr, T.R., Bleacher, J.E., Patrick, M.R., Wooten, K.M., 2015. A sinuous tumulus over an active lava tube at Kīlauea Volcano: evolution, analogs, and hazard forecasts. J. Volcanol. Geotherm. Res. 291:35–48. http://dx.doi.org/10.1016/j.jvolgeores.2014.12.002.
Pain, C.F., Clarke, J.D.A., Thomas, M., 2007. Inversion of relief on Mars. Icarus 190:478–491. http://dx.doi.org/10.1016/j.icarus.2007.03.017.
Patrick, M.R., Orr, T.R., 2011. Rootless shield and perched lava pond collapses at Kīlauea Volcano, Hawaii. Bull. Volcanol. http://dx.doi.org/10.1007/s00445-011-0505-9.
Patrick, M.R., Orr, T.R., Wilson, D., Dow, D., Freeman, R., 2011. Cyclic spattering, seismic tremor, and surface fluctuation within a perched lava channel, Kīlauea Volcano. Bull. Volcanol. http://dx.doi.org/10.1007/s00445-010-0431-2.
Patrick, M.R., Kauahikaua, J., Orr, T.R., Davies, A., Ramsey, M., 2015. Operational thermal remote sensing and lava flow monitoring at the Hawaiian Volcano Observatory. In: Harris, A.J.L., De Groeve, T., Garel, F., Carn, S.A. (Eds.), Detecting, Modelling and Responding to Effusive Eruptions. Geological Society of London Special Publication vol. 426. http://dx.doi.org/10.1144/SP426.17.
Peterson, D.W., Swanson, D.A., 1974. Observed formation of lava tubes. Stud. Speleol. 2, 209–223.
Peterson, D.W., Holcomb, R.T., Tilling, R.I., Christiansen, R.L., 1994. Development of lava tubes in the light of observations at Mauna Ulu, Kilauea Volcano, Hawaii. Bull. Volcanol. 56 (5):343–360. http://dx.doi.org/10.1007/BF00326461.
Peitersen, M.N., Crown, D.A., 1999. Downflow width behavior of Martian and terrestrial lava flows. J. Geophys. Res. 104 (E4), 8473–8488.
Peitersen, M.N., Crown, D.A., 2000. Correlations between topography and intraflow width behavior in Martian and terrestrial lava flows. J. Geophys. Res. 105 (E2):4123–4134. http://dx.doi.org/10.1029/1999JE001033.
Plescia, J.B., 2004. Morphometric properties of Martian volcanoes. J. Geophys. Res. 109, E03003. http://dx.doi.org/10.1029/2002JE002031.
Poland, M., Orr, T.R., Kauahikaua, J.P., Brantley, S.R., Babb, J.L., Patrick, M.R., Neal, C.A., Anderson, K.R., Antolik, L., Burgess, M., Elias, T., Fuke, S., Fukunaga, P., Johanson, I.A., Kagimoto, M., Kamibayashi, K., Lee, L., Miklius, A., Million, W., Moniz, C., Okubo, P.G., Sutton, A.J., Takahashi, T.J., Thelen, W.A., Tollett, W., Trusdell, F.A., 2016. The 2014–2015 Pāhoa lava flow crisis at Kīlauea Volcano, Hawai'i: disaster avoided and lessons learned. GSA Today 26 (2):4–10. http://dx.doi.org/10.1130/GSATG262A.1.
Pupysheva, N.V., Basilevsky, A.T., Ivanov, B.A., 2006. Lava tubes on the summit part of Olympus Mons volcano, Mars, and channel network at its south-east foot: morphology, depths, widths, lengths, and coefficients of sinuosity. Paper presented at 44th Vernadsky-Brown Microsymposium on Comparative Planetology, Moscow, 9–11 Oct.
Ramsey, M.S., Crown, D.A., 2010. Thermophysical and spectral variability of Arsia Mons lava flows. 41st Lunar and Planetary Science Conference, Abstract 1111. Lunar and Planetary Institute, Houston.
Richardson, J.A., Bleacher, J.E., Glaze, L.S., 2013. The volcanic history of Syria Planum, Mars. J. Volcanol. Geotherm. Res. 252:1–13. http://dx.doi.org/10.1016/j.jvolgeores.2012.11.007.
Rossi, M.J., Gudmundsson, A., 1996. The morphology and formation of flow-lobe tumuli on Icelandic shield volcanoes. J. Volcanol. Geotherm. Res. 72 (3–4), 291–308.
Rowland, S.K., Garbeil, H., 2000. Slopes of oceanic basalt volcanoes. In: Mouginis-Mark, P.J., et al. (Eds.), Remote Sensing of Active Volcanism. Geophys. Monogr. Ser. vol. 116. AGU, Washington, D.C. http://dx.doi.org/10.1029/GM116p0223.
Rowland, S.K., Walker, G.P.L., 1990. Pahoehoe and aa in Hawaii: volumetric flow rate controls the lava structure. Bull. Volcanol. 52:615–628. http://dx.doi.org/10.1007/BF00301212.
Ruff, S.W., Christensen, P.R., 2002. Bright and dark regions on Mars: particle size and mineralogical characteristics based on thermal emission spectrometer data. J. Geophys. Res. 107. http://dx.doi.org/10.1029/2001JE001580.
Self, S., Keszthelyi, L., Thordarson, T., 1998. The importance of pāhoehoe. Annu. Rev. Earth Planet. Sci. 26 (1):81–110. http://dx.doi.org/10.1146/annurev.earth.26.1.81.
Smith, D.E., Zuber, M.T., Neumann, G.A., Guinness, E.A., Slavney, S., 2003. Mars Global Surveyor Laser Altimeter Mission Experiment Gridded Data Record. NASA Planetary Data System, MGS-M-MOLA-5-MEGDR-L3-V1.0.
Stephenson, P.J., Whitehead, P.W., 1996. Field Excursion Guide, Long Lava Flows. Econ. Geol. Res. Unit Contrib. vol. 57. James Cook Univ. of North Queensland, Townsville, Australia.
Stephenson, P.J., Burch-Johnston, A.T., Stanton, D., Whitehead, P.W., 1998. Three long lava flows in north Queensland. J. Geophys. Res. 103 (B11):27359–27370. http://dx.doi.org/10.1029/98JB01670.
Swanson, D.A., 1973. Pahoehoe flows from the 1969–1971 Mauna Ulu eruption, Kilauea Volcano, Hawaii. Geol. Soc. Am. Bull. 84, 615–626.
Tanaka, K.L., Skinner Jr., J.A., Dohm, J.M., Irwin III, R.P., Kolb, E.J., Fortezzo, C.M., Platz, T., Michael, G.G., and Hare, T.M., 2014. Geologic Map of Mars, U.S.G.S. Scientific Investigations Map 3292, map scale 1:20,000,000.
Thomson, B.J., Bridges, N.T., Milliken, R., Baldridge, A., Hook, S.J., Crowley, J.K., Marion, G.M., de Souza Filho, C.R., Brown, A.J., Weitz, C.M., 2011. Constraints on the origin and evolution of the layered mound in Gale Crater, Mars using Mars Reconnaissance Orbiter data. Icarus 214 (2):413–432. http://dx.doi.org/10.1016/j.icarus.2011.05.002.
Walker, G.P.L., 1973. Lengths of lava flows. Philos. Trans. R. Soc. Lond. 274, 107–118.
Walker, G.P.L., 1991. Structure, and origin by injection of lava under surface crust, of tumuli, "lava rises", "lava-rise pits", and "lava-inflation clefts" in Hawaii. Bull. Volcanol. 53 (7), 546–558.
Walker, G.P.L., 2009. The endogenous growth of pahoehoe lava lobes and morphology of lava-rise edges. In: Thordarson, T., Self, S., Larsen, G., Rowland, S.K., Hoskuldsson, A. (Eds.), Studies in Volcanology—The Legacy of George Walker (Special Publications of IAVCEI No. 2). The Geol. Soc., pp. 17–32.

Warner, N.H., Gregg, T.K.P., 2009. Evolved lavas on Mars? Observations from southwest Arsia Mons and Sabancaya volcano, Peru. J. Geophys. Res. 108 (E10):5112. http://dx.doi.org/10.1029/2002JE001969.

Weitz, C.M., Milliken, R.E., Grant, J.A., McEwen, A.S., Williams, R.M.E., Bishop, J.L., Thomson, B.J., 2010. Mars Reconnaissance Orbiter observations of light-toned layered deposits and associated fluvial landforms on the plateaus adjacent to Valles Marineris. Icarus 205:73–102. http://dx.doi.org/10.1016/j.icarus.2009.04.017.

Wentworth, C.K., Macdonald, G.A., 1953. Structures and forms of basaltic rocks in Hawaii. U.S. Geol. Surv. Bull. 994 (98 pp.).

Werner, S.C., 2009. The global Martian volcanic evolutionary history. Icarus 201:44–68. http://dx.doi.org/10.1016/j.icarus.2008.12.019.

Whitehead, P.W., Stephenson, P.J., 1998. Lava rise ridges of the Toomba basalt flow, north Queensland, Australia. J. Geophys. Res. Solid Earth 103 (B11):27371–27382. http://dx.doi.org/10.1029/98JB00029.

Williams, K.E., Toon, O.B., Heldmann, J.L., Mellon, M.T., 2009. Ancient melting of mid-latitude snowpacks on Mars as a water source for gullies. Icarus 200 (2), 418–425.

Williams, R.M.E., Irwin III, R.P., Burr, D.M., Harrison, T., McClelland, P., 2013. Variability in Martian sinuous ridge form: case study of Aeolis Serpens in the Aeolis Dorsa, Mars, and insight from the Mirackina paleoriver, South Australia. Icarus 225:308–324. http://dx.doi.org/10.1016/j.icarus.2013.03.016.

Wilson, L., Mouginis-Mark, P.J., Tyson, S., Mackown, J., Garbeil, H., 2009. Fissure eruptions in Tharsis, Mars: implications for eruption conditions and magma sources. J. Volcanol. Geotherm. Res. 185:28–46. http://dx.doi.org/10.1016/j.jvolgeores.2009.03.006.

Witter, J.B., Harris, A.J.L., 2007. Field measurements of heat loss from skylights and lava tube systems. J. Geophys. Res. 112, B01203. http://dx.doi.org/10.1029/2005JB003800.

Wolfe, E.W., 1988. The Puu Oo Eruption of Kilauea Volcano, Hawaii: Episodes 1 Through 20, January 3, 1983, Through June 8, 1984. U.S. Geol. Surv. Prof. Paper vol. 1463.

Xiao, L., Wang, C., 2009. Geologic features of Wudalianchi volcanic field, northeastern China: implications for Martian volcanology. Planet. Space Sci. 57:685–698. http://dx.doi.org/10.1016/j.pss.2008.08.005.

Zhao, J., Huang, J., Xiao, L., 2015. Characteristics and origin of sinuous ridges in Solis Planum, Mars. 46th Lunar and Planetary Science Conference, Abstract 1897. Lunar and Planetary Institute, Houston.

Zimbelman, J.R., 1998. Emplacement of long lava flows on planetary surfaces. J. Geophys. Res. 103 (B11):27,503–27,516. http://dx.doi.org/10.1029/98JB01123.

Zimbelman, J.R., Johnston, A.K., 2001. Improved topography of the Carrizozo lava flow: implications for emplacement conditions. In: Crumpler, L., Lucas, S. (Eds.), Volcanology in New Mexico. NM Museum of Natural History and Science Bulletin vol. 18, pp. 131–136.

Zimbelman, J.R., Johnston, A.K., 2003. New precision topographic measurements of the Carrizozo and McCartys basalt flows, New Mexico. New Mexico Geol. Soc. 53rd Field ConfGeology of White Sands, pp. 121–127.

Zimbelman, J.R., Griffin, L.J., 2010. HiRISE images of yardangs and sinuous ridges in the lower member of the Medusae Fossae Formation, Mars. Icarus 205 (1), 198–210.